Development of Fluorescence-Based High-Throughput Assays for Evaluation of ADME-Tox Properties in Drug Discovery

by

Megan E. Mason

A Thesis Submitted to the Graduate
Faculty of Rensselaer Polytechnic Institute
in Partial Fulfillment of the
Requirements for the degree of
MASTER OF SCIENCE
Major Subject: Chemical Engineering

Approved:

_____
Jonathan S. Dordick, Thesis Adviser

Rensselaer Polytechnic Institute
Troy, New York

April 2008
(For Graduation May 2008)

CONTENTS

LIST OF TABLES

LIST OF FIGURES

ACKNOWLEDGMENT

Many thanks to my thesis advisor, Jonathan S. Dordick, for the time and effort put forth over the past seven years. Ever since my humble beginnings as your student and undergraduate researcher you have remained a positive role model and have shown me what is required to become a successful member of the scientific community.

Additional thanks go out to Xinxin Ding and Guoyu Ling at the Wadsworth Center (NYS Department of Health) for their guidance with the induction studies.

I would also like to acknowledge the Dordick research group for their help, support, and camaraderie. You have made my time at Rensselaer unforgettable. Thank you.

Finally, I would like to thank my family and friends. Through the good times and the bad, you have always been there when I needed you the most. I would not have made it to this point without your love and support.

ABSTRACT

The development of *in vitro* high-throughput assays to predict ADME-Tox properties early in the drug discovery process is becoming a necessity in order to reduce rapidly rising costs and high attrition rates. An increased number of hits from high-throughput lead identification studies has resulted in more compounds advancing to lead optimization and preclinical studies, only to later fail due to toxicity or poor pharmacokinetics. Early identification of compounds with poor solubility, stability, permeability, bioavailability, etc. would prevent advancement to more costly stages of the drug discovery process, or could be used as information for the optimization of the compound.

Methods to predict drug permeability are highly desirable as they can be used to estimate *in vivo* bioavailability. Animal and whole-cell models are widely used, but limited by low throughput and high cost. To counteract this problem, artificial membrane assays have been developed. Here we couple a parallel artificial membrane permeability assay (PAMPA) with a cytochrome P450 (CYP) inhibition assay to provide a new approach to estimate small molecule permeability. The advantages to this approach over traditional PAMPA include increased assay sensitivity, the ability to assess compounds that lack chromophores, and decreased assay times.

Determination of a compound's potential to inhibit or induce various CYP isoforms is critical to preventing drug-drug interactions (DDIs). While many *in vitro* assays have been developed to measure CYP inhibition, primary hepatocytes remain the FDA-preferred method of measuring CYP induction. These assays are expensive and highly variable due to the frequency of certain CYP polymorphisms. Reporter gene assays can be used to measure induction by inserting the regulatory elements from a CYP gene upstream of a gene that expresses a fluorescent protein or luciferase. In this study, H4IIE cells are transfected with various constructs that differ in the number of drug response elements (DREs) and type of promoter. These cells are then exposed to an inducer and the effect on gene expression is measured using a standard fluorescence plate reader.

1. Introduction

1.1 Overview of Drug Discovery and ADME-Tox

The current challenges faced by the pharmaceutical industry in bringing a drug to market are not trivial. Advancing a drug through the discovery process to FDA approval is an increasingly rare and expensive occurrence. The cost to bring a drug to market is about $0.9-1.8 billion, requires almost nine years of research, and only has a success rate of about 0.1% (Kumar, 2006). In 2007, only 17 new molecular entities (NMEs) were approved by the FDA (Hughes, 2008) as compared to 39 NMEs approved ten years ago (Figure 1-1).

High-throughput screening (HTS) has been invaluable to the drug discovery process in that thousands of compounds can be screened on a daily basis from chemically-diverse libraries containing upwards of 1-2 million compounds (Kariv, 2002). Robotic liquid handling systems, sensitive detection systems, and miniaturized assay formats (e.g. microwell plates, microarrays) have contributed to significant reductions in lead identification times. While this may be viewed as a positive achievement, it has also led to an increase in the number of compounds that are advanced to costly pre-clinical trials. The failure of compounds in later stages of clinical trials has emphasized the need to improve early identification of potential issues related to toxicology, stability, solubility, bioavailability, and other pharmacokinetic properties. Early identification of adverse adsorption, distribution, metabolism, elimination, and toxicity (ADME-Tox) properties would not only increase the speed that drugs are brought to market, but would also increase the rate of success (McGee, 2005; Kerns,

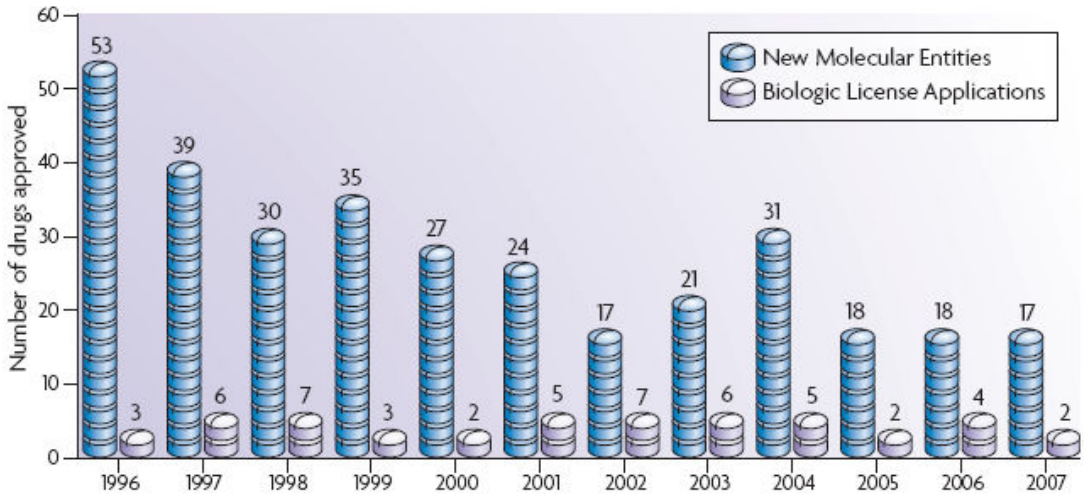

Figure 1-1 FDA drug approvals

(Hughes, 2008)

2003). Similarly, compounds that have been identified as leads could also benefit from early optimization of ADME-Tox properties before they enter late-stage clinical trials.

The majority of HTS screens in drug discovery measure some form of biological activity or molecule such as enzyme inhibition, protein modification (e.g. phosphorylation by kinases), and nucleic acid or protein quantization (Kumar, 2006). A wide range of assay techniques exist that incorporate a variety of detection methods. Fluorescence-based assays usually utilize a biocatalytic transformation to alter the fluorescence of a substrate or involve the presence of a molecule that quenches the fluorescent signal in response to enzymatic activity. Bioluminescence assays are typically used for ATP-dependent reactions and therefore are commonly used to measure kinase activity. Luciferase reacts very efficiently with ATP to produce light that can be measured with a luminometer or CCD camera. Fluorescence and luminescence are also commonly used in reporter gene assays where the expression of the fluorescent protein or luciferase is produced under specific conditions (Lang, 2006). Immunoassays use labeled antibodies to detect a molecule of interest with extremely high specificity. The major drawback to these types of assays is that multiple washing steps are usually required. Radioactive assays, such as the scintillation proximity assay, are commonly used in industry due to the fact they utilize a generic substrate (Zheng, 2004). A major drawback to this assay is that radioactive materials may not be desirable due to strict handling protocols and short half-lives. If structural characterization is needed or complex mixtures are being analyzed, nuclear magnetic resonance (NMR) spectroscopy or combined chromatographic/mass spectroscopy techniques can be employed (Dierks, 2001). While these techniques are not traditionally high-throughput, many advances are

being made to increase the speed and therefore the number of samples that can be analyzed in a reasonable amount of time (Kassel, 2004).

Development of a successful HTS assay must take into account the overall required assay time, reproducibility, robustness, and cost. Assays should be amenable to scale-down to different microwell plate formats and adaptable to automated robotic systems typically used in industry. The number of assay steps as well as the complexity and safety of each of these steps should be considered. For example, steps that require filtration or separation should be avoided, as well as toxic substrates or the use of radioactive materials (these are typically costly and require special handling).

The ability to assess the ADME-Tox profiles of new compounds early in the drug discovery process is dependent upon successful development of cheap, fast, and reliable assays. Many ADME-Tox properties that these assays would target are affiliated with cytochrome P450s (CYPs), which are a large and diverse superfamily of heme proteins responsible for oxidative metabolism of both endogenous and exogenous compounds (Ortiz de Montellano, 1995). CYPs are found primary in liver tissue, but are also present in a variety of other mammalian tissues including the kidney, lung, brain, and small intestine (Seliskar, 2007) as well as in a variety of organisms (fish, plants, yeast, and bacteria). CYPs are usually membrane-bound proteins located in the inner membrane of mitochondria (Omura, 2006) or the endoplasmic reticulum (ER) and possess the capability to metabolize multiple substrates. The most important isoforms with respect to human drug metabolism are CYP3A4, CYP2D6, and CYP2C9 (Kariv, 2002; Thummel, 1998). It is estimated that upwards of 50% of drugs used on humans undergo some form of CYP3A4-mediated metabolism.

Another ADME-Tox property that could be evaluated early in the drug discovery process is drug absorption. Caco-2 (a human colon adenocarcinoma cell line) and Madin-Darby canine kidney (MDCK) cells are both immortalized cell lines widely used to assess drug permeability (Hidalgo, 2001; Ingels, 2003; Shah, 2006). Both cell lines differentiate into monolayers of polarized epithelial cells which mimic the gastrointestinal lining. These cell lines are subject to long culture times (up to 21 days) which make these assays both labor intensive and expensive. An alternative to cell models are artificial membrane assays which can predict the passive transcellular permeability (Kariv, 2002). These assays are much more amenable to high-throughput screening and are less expensive than their whole cell counterparts, but the major argument against them is their inability to assess passive paracellular or active transport.

1.2 Goals of this work

The focus of this work is to develop and validate two high-throughput assays that can be implemented early in the drug discovery process to assess ADME-Tox properties of new chemical entities (NCEs). First, an artificial membrane permeability assay is multiplexed with CYP inhibition assays to predict the passive permeability of drugs. This method takes advantage of the sensitivity of the fluorescence-based CYP inhibition assay allowing for permeability assessment of poorly soluble compounds as well as molecules lacking a suitable chromophore (required for traditional UV/Vis detection). Additionally, the impact of permeability on a compounds inhibition profile can be assessed. This approach is not limited to just inhibition assays and should be extendable to a variety of other fluorescence or luminescence-based assays.

The second part of this work involves the development of a reporter gene assay to measure CYP1A1 induction. Green fluorescent protein (GFP) is placed under the control of the *CYP1A1* gene's regulatory elements, therefore resulting in protein expression when the host cell is exposed to an inducer. The effect on induction caused by changing the enhancer and promoter elements is also explored. Finally, future directions for this work are also suggested.

2. The Combined PAMPA/CYP Inhibition Assay

2.1 Introduction

An emerging trend in drug discovery research is to assess ADME/Tox properties of drug candidates earlier in the discovery process. To facilitate this demand in a time-efficient and economical manner, the development of cheap, fast, high-throughput *in vitro* screening assays is required. One method of achieving this requirement is to multiplex assays (O'Brien, 2005). Combining assays allows for lower consumption of materials, reduced assay time, and potentially more insight to the *in vivo* effect of a drug.

Oral administration of a therapeutic is the preferred route due to convenience and high patient compliance. Therefore, drug absorption is a critical factor and represents a key barrier in drug development. Drug permeability across the intestinal epithelium is a complex process involving multiple pathways including passive transcellular and paracellular diffusion, carrier-mediated transport and efflux, and vesicular transport (Shah, 2006). It is widely accepted that the majority of drugs are absorbed via passive diffusion, and even for compounds with multiple mechanisms of transport, passive diffusion will dominate due to receptor saturation at clinically administered doses (Kansy, 2004).

In addition to permeability, there are many other ADME properties that should be evaluated early in the drug discovery process. CYP450 inhibition is a major cause of drug-drug interactions due to the reduced ability to metabolize a drug into its inactive form, which can lead to a cytotoxic event (Cupp, 1998). Early identification of inhibitors can prevent compounds from proceeding further through the costly drug

discovery process and may even allow for further modification of a compound until a suitable safety profile is achieved.

A variety of *in vivo*, *in vitro*, and *in silico* methods exist for measuring or predicting the permeability of compounds (Hidalgo, 2001) and are summarized in Table 2-1. Traditional *in vivo* methods include use of whole animals to make differential urinary excretion measurements. These methods have the benefit of including passive and active transport mechanisms but are expensive and low-throughput. Additionally, they do not lead to the identification of which mechanism serves as the primary mode of transport. *In vitro* methods include the use of excised tissue samples, intestinal perfusion techniques, whole-cell techniques (Caco-2, MDCK, and HT29), and artificial membrane methods (IAM, PAMPA). These methods have distinct advantages and disadvantages, but are amenable to a high-throughput format which makes them increasingly popular from a drug discovery perspective. Finally, *in silico* tools to predict permeability such as prediction of logP (partition coefficient of a neutral compound in octanol-water) and logD (distribution coefficient of all ionized species of a compound in octanol-water) from QSTR models are becoming increasingly popular. The major criticism of this approach, however, is that the quality of results strongly depends on the reliability and diversity of the data sets used to train these models. There has been only limited success in developing a model that accurately predicts permeability values for a wide range of compounds.

Table 2-1 Methods used to assess compound permeability

	Methods	Disadvantages	Advantages
in vivo	whole animal models	Incorporates all transport mechanisms	Expensive, time-consuming, labor-intensive
		Animals can be reused for pharmacology/toxicology studies	No mechanistic information
			Low-throughput
in vitro	excised tissues	Can measure permeability for different insestinal segments	Low viability
	intestinal perfusion	Can study segmental differences in permeability	Low viability
		Elucidation of transport mechanisms	Large amounts of compound needed
	whole-cell models (Caco-2, MDKC)	High-throughput	Expensive, long-culture times, labor-instensive
		Possess features similar to intestinal cells	High inter-laboratory variability
		Multiple transport mechanisms	No regional intestinal differentiation
	artificial membranes (PAMPA, IAM)	Inexpensive, high-throughput	No paracellular and active transport
		Reproducibile	Detection limitations (LC/MS, UV/Vis)
in silico	QSTR (logP, logD)	Inexpensive, high-throughput, fast	Unreliable data
		Predictive - can be estimated before compounds are made	Hard to create diverse training sets

The parallel artificial membrane permeability assay (PAMPA) was first introduced by Kansay *et al.* ten years ago as a method to predict passive transcellular diffusion of a compound through a lipid membrane (Kansy, 1998; Avdeef, 2005). The original method involves impregnating a 96-well microtiter plate containing a hydrophobic filter membrane with a 1-20% (w/v) solution of lecithin (phosphatidylcholine) in dodecane. The well-plate is then used to create a "sandwich" where a drug solution of known concentration (termed the donor well) is allowed to diffuse into a clean buffer solution (termed the acceptor well). After a defined period of time, the well plates are separated and the concentration of drug in each well is determined spectrophotometrically.

Since PAMPA's introduction, there has been substantial effort in modifying the assay to create new adaptations of PAMPA to measure drug absorption. The traditional lecithin-PAMPA method was based on the fact that phosphatidylcholine is the major component of cell membranes. Several groups have modified PAMPA to include other membrane components such as cholesterol or have mimicked the phospholipid composition found in specific tissues. These variations include biomimetic PAMPA (BM-PAMPA) and blood-brain barrier PAMPA (BBB-PAMPA) which is based on porcine brain tissue (Sugano, 2002; Di, 2003). *n*-Hexadecane PAMPA (HDM-PAMPA) involves the partitioning of drugs between a membrane containing just the inert organic solvent (Wohnsland, 2001). The introduction of sink conditions (DS-PAMPA) has been shown to improve PAMPA correlations with human absorption (Avdeef, 2005). A pH gradient is used as the first sink condition to replicate the wide pH range (pH 5-8) present in the intestine and therefore represent all relevant absorption ionization states. The second gradient condition involves the addition of surfactant to the acceptor well,

which traps test compounds and drastically reduces assay time. Other methods, including shaking or stirring wells to decrease the aqueous boundary layer (ABL) have also been used to reduce assay time from about 15 h to 30 min (Ruell, 2003; Nielsen, 2004; Avdeef, 2004).

While PAMPA has been shown to reasonably estimate human absorption in a high-throughput manner, there are limitations to its application. The preferred detection method is UV absorbance, which is dependent on a molecule having a suitable chromophore. Molecules with poor chromophores require higher concentrations that may result in solubility limitations in aqueous buffers. Moreover, it has been shown that up to 40% of pharmaceutical compounds dissolved in DMSO have an actual concentration 20% lower than the expected value due to solubility issues. The same problem is evident for up to 80% of compounds dissolved in aqueous buffers (DeWitte, 2006). Increasing test compound concentration further increases solubility issues and can result in drastically overestimated concentrations.

An increasingly popular method to overcome the issue of detection sensitivity is to couple PAMPA with different mass spectrometry techniques (Balimane, 2005; Mensch, 2007). While this approach has been successful, the increased time and cost to prepare and run samples detracts from capacity of PAMPA to be run as a high-throughput assay. Incorporating LC/MS does not result in any more information about a compound than is obtained from traditional PAMPA, therefore making it difficult to justify the increase in assay time.

We propose that PAMPA can be coupled to an alternative sensing system that involves fluorescent or luminescent-based assays to take advantage of the sensitivity of

these detection methods, maintain a high-throughput capacity, and obtain more information about the test compounds of interest. In principle PAMPA can be coupled to a large variety of receptor, enzyme, or whole cell assays that are commonly used in drug discovery to identify the potency of a compound, as well as to assess the influence of permeability on bioavailability.

The primary goal of this study was to demonstrate that a combination of permeability and enzyme kinetic assays may be used to overcome some of the aforementioned limitations and to assess simultaneously multiple pharmacologically-relevant properties. Specifically, we have combined PAMPA with several different cytochrome P450 inhibition assays (CYP3A4, 2C9, and 2D6) to evaluate the passive permeability of known inhibitors. The ability of the assay to correctly identify and rank the potency of inhibitors was assessed. The measured permeability values were compared to those obtained by traditional PAMPA and the widely accepted Caco-2 permeability assays.

2.2 Materials and Methods

2.2.1 Materials

All test compounds were obtained from Sigma-Aldrich (St. Louis, MO). L-α-phosphatidylcholine (egg, chicken) was obtained from Avanti Polar Lipids (Alabaster, AL). Dodecane (99%) and reagent grade methanol (MeOH) were purchased from Acros Organics (Morris Plains, NJ). Reagent grade dimethyl sulfoxide (DMSO) was from Fisher (Pittsburg, PA). Phosphate buffered saline (PBS) powder was obtained from Sigma and was prepared according to the suppliers instructions (adjusted to pH 6.2, 7.4,

or 8.0 with phosphoric acid or sodium hydroxide). Sodium acetate buffer (50 mM) was prepared with reagent grade glacial acetic acid from Fisher and adjusted to pH 5.0. The donor plate was a 96-well hydrophobic PVDF filter plate (Multiscreen®, catalog MAIPNTR10, 0.45 μm) and the acceptor plate was a 96-well clear polystyrene plate (Multiscreen®, catalog MATRNPS50) from Millipore (Bedford, MA). A 96-well quartz plate was used for UV measurements.

Vivid® CYP450 Screening Kits for CYP3A4, 2C9, and 2D6 (catalog P2857, P2860, and P2972, respectively) were obtained from Invitrogen (Carlsbad, CA). White 96-well plates (Costar®) from VWR (South Plainfield, NJ) were used for fluorescence measurements.

2.2.2 PAMPA procedure

For the UV detection of PAMPA compounds, 5 mg/mL solutions were prepared in DMSO and then 10 μL were diluted in 4 mL of appropriate buffer (pH 5.0, 6.2, 7.4, and 8.0) for a final concentration of 25 μg/mL. The UV/Vis profiles for eight compounds were determined over the range of 200 to 500 nm using a Shimadzu UV-2401PC UV/Vis spectrophotometer (Shimadzu, Columbia, MD). Buffer (300 μL of pH 7.4) was added to each well of the acceptor plate. The donor plate was prepared by adding 5 μL of 1% (w/v) lipid solution (lecithin in dodecane) and immediately adding 150 μL of the appropriate drug solution. All drug solutions were added in triplicate for each pH. The plates were carefully placed together with the aqueous acceptor being on the bottom, the organic membrane in the middle, and the aqueous donor containing the test compounds on the top. The sandwiched plates were covered and sealed to minimize

evaporation. The plates were left to incubate undisturbed at room temperature overnight (15-18 hours). The plates were separated and 150 μL of the solution in the acceptor wells was transferred to a quartz plate and the absorbance was determined using a Perkin Elmer HTS 7000 Bio Assay plate reader (Perkin Elmer, Waltham, MA) at 260, 280, and 325 nm.

The effective permeability (P_e) was determined using Eqs. 1 and 2:

$$\log P_e = \log\left\{C \times -\ln\left(1 - \frac{[\mathrm{TC}]_{\mathrm{Theor.\ Eq.}}}{[\mathrm{TC}]_{\mathrm{Acceptor}}}\right)\right\} \quad (1)$$

$$C = \frac{V_D \times V_A}{(V_D + V_A)\mathrm{Area} \times \mathrm{Time}} \quad (2)$$

where [TC] is the concentration of the test compound in the acceptor plate or at the theoretical equilibrium (the concentration of drug if the acceptor and donor wells were mixed together), V_D is the volume in the donor well (0.15 cm^3), V_A is the volume in the acceptor well (0.30 cm^3), the area is the active surface area of the membrane (0.24 cm^2), and the time is the incubation time for the assay in seconds. For UV detection the drug concentration ratio is replaced with the ratio of absorbance. Many other models exist for calculating the effective permeability and take into account more variables such as membrane retention of the drug, corrections for PAMPA's inability to take into account passive paracellular diffusion, and corrections for the presence of an unstirred water layer. Here we consider the simplest case, but bear in mind that our approach could be easily modified to use any of models.

2.2.3 PAMPA/CYP inhibition procedure

The PAMPA procedure is identical to that described above, with the exception of initial compound concentration. Stock solutions (10 mM) were prepared in DMSO or MeOH depending on compound solubility. Subsequent dilutions were made in buffer to ensure that the final DMSO or MeOH concentration was less than 0.1% in order to avoid significant solvent inhibition of CYPs as suggested by the manufacturer's protocol supplied with the Vivid CYP450 screening kit. The final concentration of the test compound was dependent upon the IC_{50} value to ensure measurements were within the linear range of inhibition. These solutions were prepared at three pH values (5.0, 7.4, and 8.0). If the IC_{50} was known, the test compounds were diluted to 7.5-fold higher than the known IC_{50} concentration. This takes into account the 3-fold and 2.5-fold dilution from the PAMPA and inhibition assays, respectively. If the IC_{50} was unknown, solutions were prepared at a final concentration of 5 μM. Additionally, theoretical equilibrium solutions, or the solution that would be obtained if the acceptor wells and donor wells were mixed together, were prepared at pH 7.4 and 2.5-fold higher than the chosen final concentration and were used for the inhibition assay only.

After the PAMPA incubation, 40 μL of the test compound solution from the acceptor plate was transferred to a white 96-well plate. Theoretical equilibrium solutions (40 μL) were added to the last three columns of the plate. A positive inhibition control replaced the test compound solution in triplicate for each CYP isoform (a final concentration of 10 μM ketoconazole for CYP3A4, 10 μM sulfaphenazole for CYP2C9, and 1 μM quinidine for 2D6). Additionally, a negative inhibition control (no test compound), fluorescence background control (buffer and fluorogenic substrate only),

and a buffer-only control were added in triplicate. The manufacturer protocol supplied with each Invitrogen kit was followed to prepare to enzyme and its corresponding fluorogenic substrate. Enzyme solution (50 μL) was added to each well and allowed to incubate with the test compounds for 20 min. Substrate solution (10 μL) was added and either read in kinetic mode in the plate reader for 30 min or allowed to incubate for 20 min. If an endpoint-only assay was desired, 10 μL of stop solution (identical to compound and concentration used for the positive inhibition controls, e.g. 10 μM ketoconazole for CYP3A4) was added to each well and then read in the plate reader. For CYP3A4 and 2C9 the excitation and emission wavelengths were 485 nm and 535 nm, respectively. For CYP2D9, the excitation wavelength was 405 nm and the emission wavelength was 465 nm.

To calculate the effective permeability based on the inhibition results, Eq. 1 was modified to Eq. 3:

$$\log P_e = \log\left\{C \times -\ln\left(1 - \frac{\mathrm{RFU}_{\mathrm{Acceptor}}}{\mathrm{RFU}_{\mathrm{Theor.\,Eq.}}}\right)\right\} \tag{3}$$

The ratio is inverted because an increase in drug concentration will result in a decreased response. Additionally, the percent inhibition of a compound was calculated using Eq. 4:

$$\%\,\mathrm{Inhibition} = \left(1 - \frac{\mathrm{RFU\ of\ test\ compound\ at\ theoretical\ equilibrium}}{\mathrm{RFU\ of\ negative\ inhibition\ control}}\right) \times 100\% \tag{4}$$

The percent inhibition can be related to the IC_{50} and compound concentration by the Hill equation:

$$\mathrm{Response} = 1 - \%\mathrm{Inhibition} = \mathrm{Bottom} + \frac{(\mathrm{Top} - \mathrm{Bottom})}{1 + 10^{(\log \mathrm{IC}_{50} - X)\mathrm{HillSlope}}} \tag{5}$$

where Top and Bottom are the upper and lower limits (chosen to be 100% and 0%), *X* is the log of the concentration of the test compound used, and the Hill slope defines the steepness of the curve. Most inhibitory systems exhibit behavior characteristic of a Hill slope approximately equal to -1.

2.3 Results and Discussion

2.3.1 Traditional PAMPA

The UV/Vis profiles were obtained for eight test compounds that have been previously well characterized using the PAMPA procedure. Table 2-2 shows the maximum absorbance wavelengths obtained for each compound as well as the corresponding absorbance. In Figure 2-1 the profiles are plotted against each other over the range of 200 to 500 nm with the dashed lines passing through the curves at 260 nm and 280 nm. The large variation in absorbance values obtained within the linear range of the detector is problematic. At the compound concentration used (25 μg/mL), acetylsalicylic acid does not significantly absorb within the selected range. This demonstrates the limitations of using UV/Vis spectroscopy as the endpoint measurement. All compounds being assessed by this method must have a suitable chromophore and may need to be prepared at very high concentrations to achieve the minimum linear range of detection. Because we are measuring permeability, this concentration requirement is increased, as enough of the drug must permeate through the membrane before UV/Vis can be employed. For low permeability compounds with weak chromophores this implies large concentrations and long incubation times are necessary.

The increase in incubation time significantly impacts the permeability measurement. For compounds that reach equilibrium quickly, the long incubation time will decrease the effective permeability calculated by Eq. 1. This emphasizes the need for a more sensitive detection method so that overall assay time can be significantly decreased, thus increasing the accuracy of permeability assessment and overall throughput of the assay.

Table 2-2 Maximum absorbance for selected compounds

Compound	MW (g/mol)	Concentration (μM)	λ_{max} (nm)	Absorbance
Verapamil	454.60	54.99	278	0.275
Theophylline	180.16	138.76	271	1.066
Propanolol	259.34	96.40	290	0.504
Ketoprofen	254.28	98.32	260	1.344
Furosemide	330.75	75.59	277	1.578
Caffeine	194.19	128.74	273	1.377
Carbamazepine	236.17	105.86	285	1.394
Acetylsalicylic acid	180.16	138.77	-	-

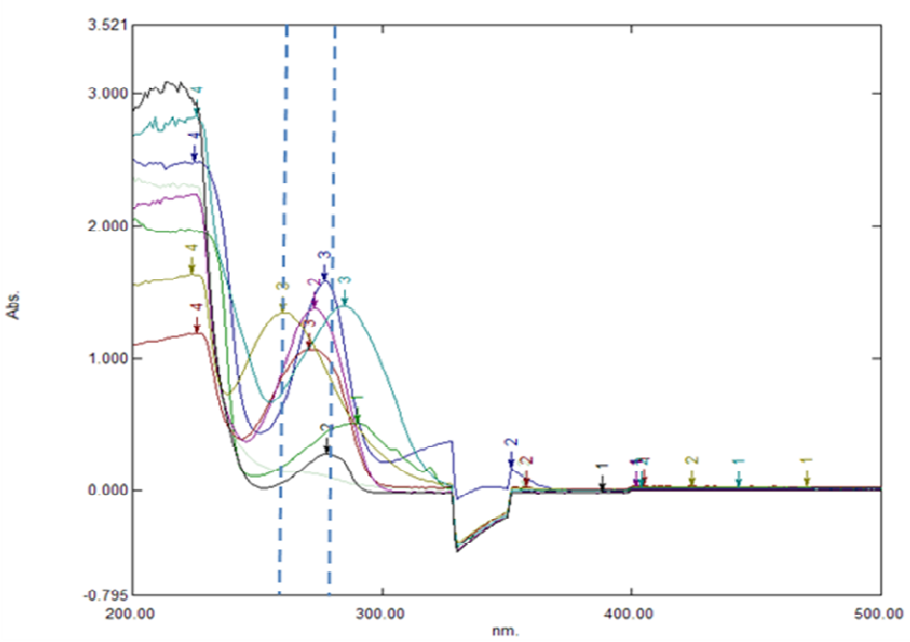

Figure 2-1 UV/Vis profiles for selected compounds

2.3.2 Mathematical limitations of the PAMPA/inhibition assay

For compounds with known IC_{50} values, the PAMPA/inhibition assay should be performed using a final test compound concentration approximately corresponding to the IC_{50}. This ensures that the compound is within the approximate linear range of inhibition. The acceptable range of concentration depends on the Hill slope that best describes a compounds inhibitory behavior given by Eq. 5. The general behavior of the Hill equation for various Hill slopes is shown in Figure 2-2.

Coupling Eq. 5 with the permeability equation (Eqs. 1 or 3), the minimum measurable permeability can be calculated based on the minimum concentration that must be in the acceptor well that produces a 10-20% inhibitory response. Table 2-3 provides guidelines to the acceptable concentration range and minimum permeability that can be calculated using the combined PAMPA/inhibition approach. The minimum concentrations corresponding to a response of 10-20% were found by inserting various Hill slopes and a theoretical IC_{50} of 1 μM into Eq. 5 and then solving for *X*. The same approach was used to find the maximum concentration corresponding to a response of 80-90%.

An IC_{50} of 1 μM was selected arbitrarily as it simplifies the math and allows for easily calculation of a concentration range where this method can be applied. The concentration range for any other IC_{50} is found by multiplying the IC_{50} by the minimum and maximum concentration in Table 2-3. For example, to accurately measure the permeability of a compound with an IC_{50} of 0.5 μM and a Hill slope of -1, the test compound could be prepared at any concentration 4-fold higher or lower than the IC_{50}

(between 0.125 and 2 μM). Therefore, if the IC_{50} is approximately known, the combined PAMPA/inhibition method will still be able to calculate the permeability.

To calculate the minimum measurable permeability, the minimum concentrations were plugged into Eq. 1 along with the selected IC_{50} of 1 μM. For shallow inhibition curves, this approach can be used to measure a wide range of concentrations (about 80-fold higher or lower than the IC_{50}) and can accurately detect low-permeability compounds down to 0.1×10^{-6} cm s^{-1}. For steep inhibition profiles, it is recommended that compounds with a calculated permeability less than 2×10^{-6} cm s^{-1} be classified as "low-permeability" as a slight shift in the concentration can lead to significant errors in the calculated value.

There is no limit to the theoretical maximum permeability using this approach as Eqs. 1 and 3 will approach an infinite value; however, Eq. 4 must be used to ensure that the percent inhibition is higher than 10-20%. If the selected concentration for the IC_{50} or theoretical equilibrium produces a response less than this, the measured permeability will be artificially higher than the actual permeability. Likewise, if a compound shows greater than 80-90% inhibition, the selected concentration for the theoretical equilibrium is much greater than the IC_{50} and falls out of the linear inhibition range. This will also result in calculation of an inaccurate permeability.

Table 2-3 Limits to the PAMPA/inhibition assay

	Linear Range: 20-80% (>99.5% linearity)				Linear Range: 10-90% (>99% linearity)			
Hill Slope	Min Conc.	Max Conc.	Min Perm @15h (10^{-6} cm s^{-1})	IC_{50} Range	Min Conc.	Max Conc.	Min Perm @15h (10^{-6} cm s^{-1})	IC_{50} Range
-0.5	0.06	16	0.50	16	0.01	81.1	0.09	81
-1	0.25	4	2.22	4	0.11	9	0.91	9
-1.5	0.40	2.5	3.94	2.5	0.23	4.3	2.03	4.3
-2	0.50	2	5.35	2	0.33	3	3.12	3

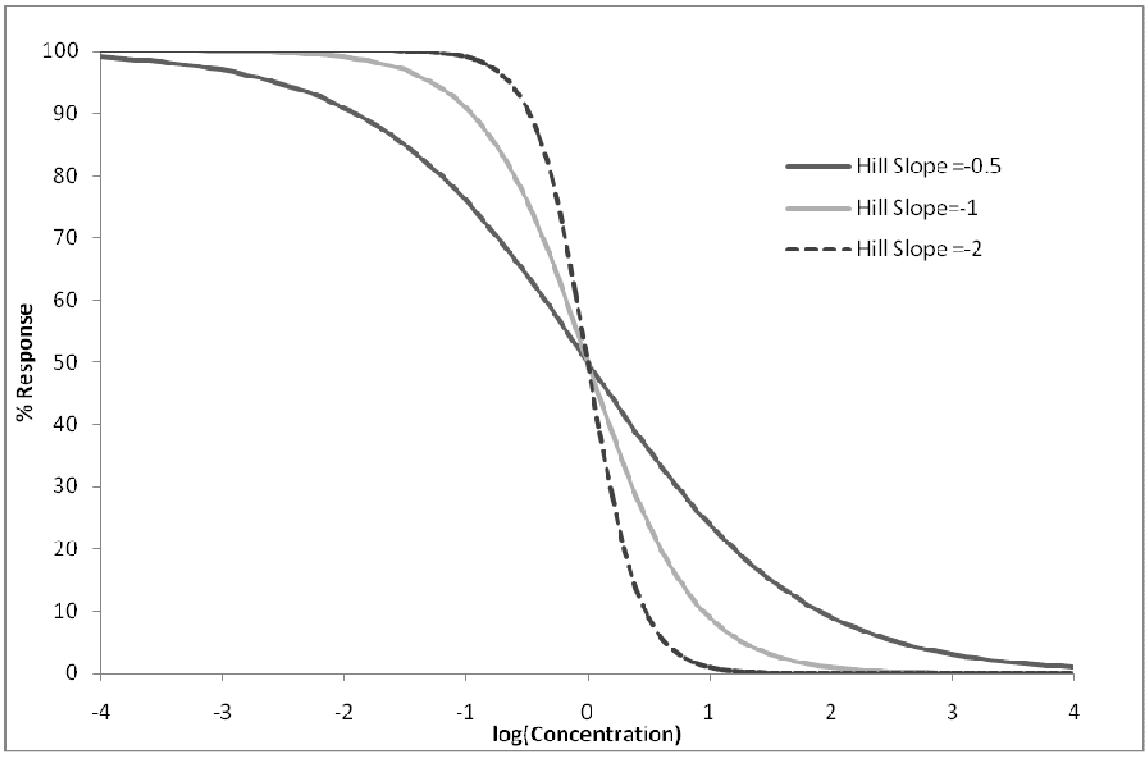

Figure 2-2 Shape of inhibition curves for various Hill slopes

2.3.3 Estimation of permeability from the combined PAMPA/inhibition assay

Table 2-4 summarizes the percent inhibition obtained for various compounds tested as inhibitors of CYP3A4, 2C9, and 2D6. For compounds with unknown IC_{50} values, the concentrations were either guessed and are italicized in Table 2-4. Using the limitations presented in Table 2-3, compounds can immediately be classified as weak or strong inhibitors at the selected concentrations if they fall outside the linear range of inhibition and the concentration can be adjusted accordingly. Eq. 3 can be used to calculate the effective permeability for the remaining compounds that fall within the linear range of inhibition. For CYP3A4, tamoxifen is not considered inhibitory at the experimental concentration. The effect on the permeability calculation can be seen in Figure 2-3 where tamoxifen exhibits unusually high permeability and large error. Similarly for CYP2C9, fluconazole, amiodarone, and isonizaid are identified as non-inhibitors at the experimental concentrations and produce nearly identical permeability results to tamoxifen. Amiodarone, sulfaphenazole, and isoniazid do not inhibit CYP2D6 at the assay concentrations.

The experimental P_{app} values obtained from the PAMPA/3A4 inhibition assay are shown in Table 2-5. A summary of the experimental results are compared to reported literature values available for several compounds at various pH's. Discrepancies are observed between literature values available for identical compounds which is presumably due to the large number of variables associated with traditional PAMPA. Incubation time, compound concentration, individual well stirring, lipophilic sinks in the acceptor well, and pH gradients between the donor and acceptor wells are all variables that significantly impact the measured permeability. Guidelines for PAMPA

that address each of these variables have been recently published in order to promote consistancy of results (Avdeef, 2007). The P_{app} values obtained using the PAMPA/inhibition method fall within the range of the literature values.

Table 2-4 Percent inhibition of select CYP inhibitors

	CYP3A4 Inhibition		CYP2C9 Inhibition		CYP2D6 Inhibition	
Compound	Conc. (μM)	%Inhibition	Conc. (μM)	%Inhibition	Conc. (μM)	%Inhibition
Quinidine	*5*	23%	-	-	0.05	73%
Verapamil	3.2	42%	-	-	-	-
Tamoxifen	5	7%	-	-	-	-
Isoniazid	*5*	15%	*0.5*	0%	*5*	9%
Miconazole	20	45%	1	28%	2.5	19%
Erythromycin	4	28%	-	-	-	-
Ketoconazole	0.5	82%	*5*	22%	*5*	38%
Fluconazole	-	-	*0.5*	0%	-	-
Amiodarone	-	-	*0.5*	0%	*5*	0%
Sulfaphenazole	-	-	0.5	31%	*5*	9%
Clotrimazole	-	-	0.5	37%	-	-
Nicardipine	-	-	-	-	6	65%

Table 2-5 Experimental permeability values and literature comparison

Compound	Caco-2[a]	F_a[b]	Experimental P_e			Kerns *et al.* P_e[c]		Zhu *et al.* P_{app}[b]	
	P_{app}	(%)	pH 5	pH 7.4	pH 8	pH 4	pH 7.4	pH 5.5	pH 7.4
Quinidine	20.42	80	7.0	8.5	11.2	0.2	4.2	6.0	10.9
Verapamil	26.30	98	4.0	6.9	9.0	1.7	14.0	9.7	7.4
Miconazole	-	99	3.6	4.1	4.6	-	-	0.7	0.0
Erythromycin	3.72	35	5.7	6.1	6.8	0.0	7.9	0.1	0.1
Ketoconazole	-	75	0.9	1.0	1.1	1.7	9.1	3.3	1.2

[a] Caco-2 P_{app} (cm s^{-1} x10^6) obtained from DrugBank (http://www.drugbank.ca)

[b] F_a, P_{app} (cm s^{-1} x10^6) values cited from Zhu *et al.* Eur. J. Med. Chem. 37 (2002)

[c] P_{app} (cm s^{-1} x10^6) values cited from Kerns *et al.* J. Pharm. Sci 93 (2004)

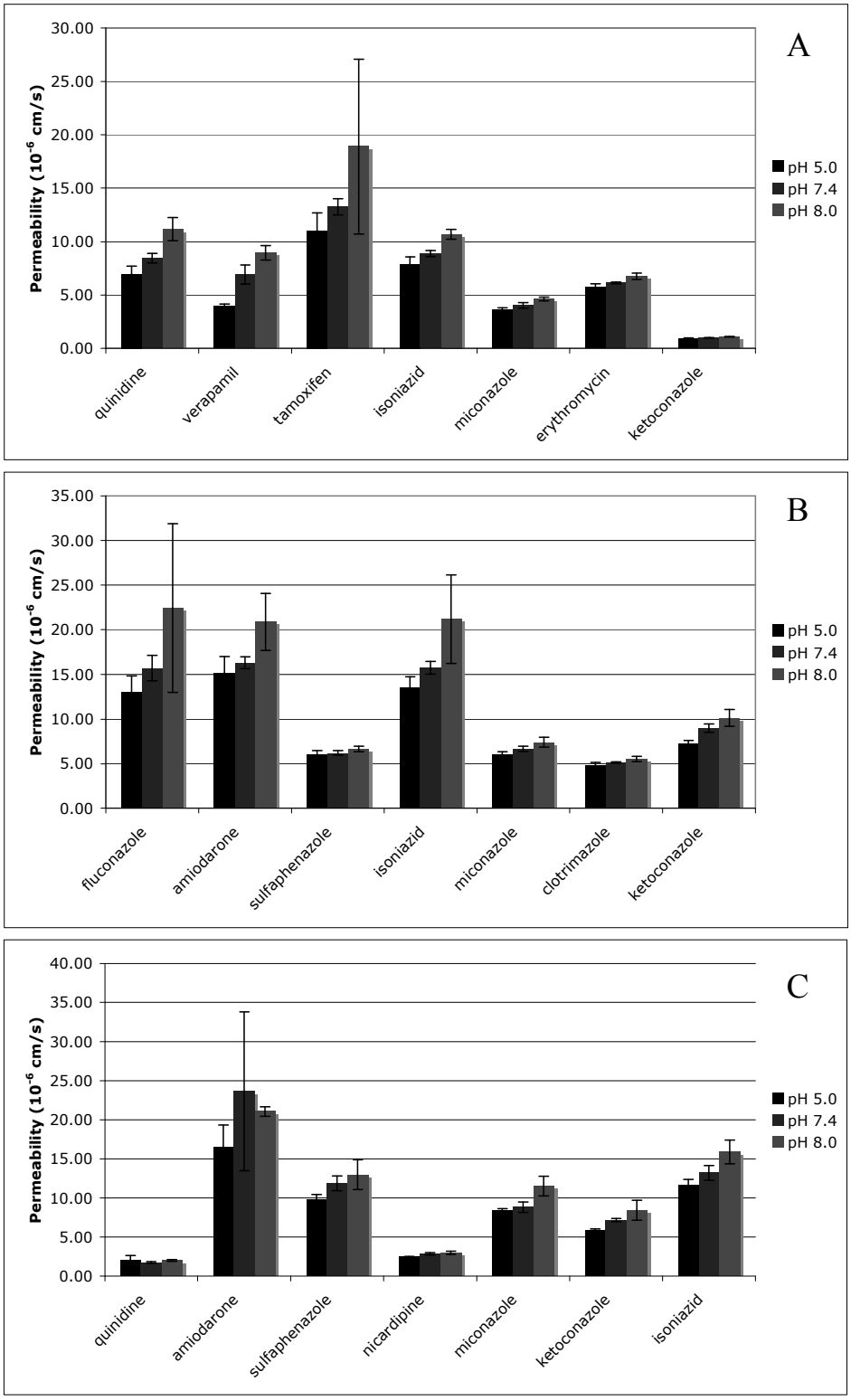

Figure 2-3 Calculated permeability from the PAMPA/inhibition assays

A) CYP3A4 inhibition B) CYP2C9 inhibition C) CYP2D6 inhibition

2.3.4 Permeability and the dose response of ketoconazole

To confirm that permeability can be determined over the nearly linear range of inhibition, the permeability of ketoconazole was measured at 12 different concentrations from 0.05 μM to 10 μM at an incubation time of 18 hours using the PAMPA/CYP3A4 inhibition procedure. Literature IC_{50} concentrations for ketoconazole range from about 0.05 to 0.5 μM depending on the detection method employed. Figure 2-4 shows that the calculated permeability will hold constant at approximately 1.7 x 10^{-6} cm s^{-1} from about 0.2 – 1.25 μM which is consistent with Table 2-2. Outside of the linear response range, the permeability becomes artificially large as the fluorescence response for the drug in the acceptor wells approach the fluorescence of the corresponding theoretical equilibrium.

The effect of permeability on a dose response curve is shown in Figure 2-5. After the background fluorescence is subtracted, the fluorescence response is normalized by the response at 0.05 μM. The data is then fit by minimizing the sum-of-squares with equation 4 and allowing the IC_{50} and Hill slope to vary. Permeability is calculated by inserting the corresponding IC_{50} values for the PAMPA curve and the theoretical equilibrium curve into equation 1. When the dose response curves for ketoconazole are compared in Figure 2-5, the concentration shift corresponds to the expected permeability of approximately 1x10^{-6} cm/s.

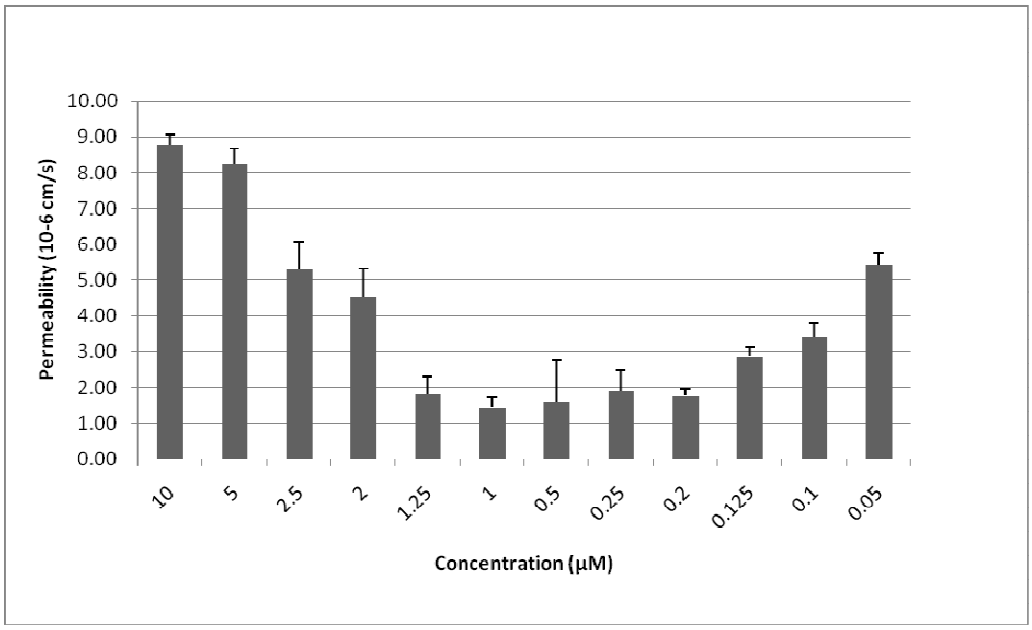

Figure 2-4 Effect of concentration of the calculated permeability of ketoconazole

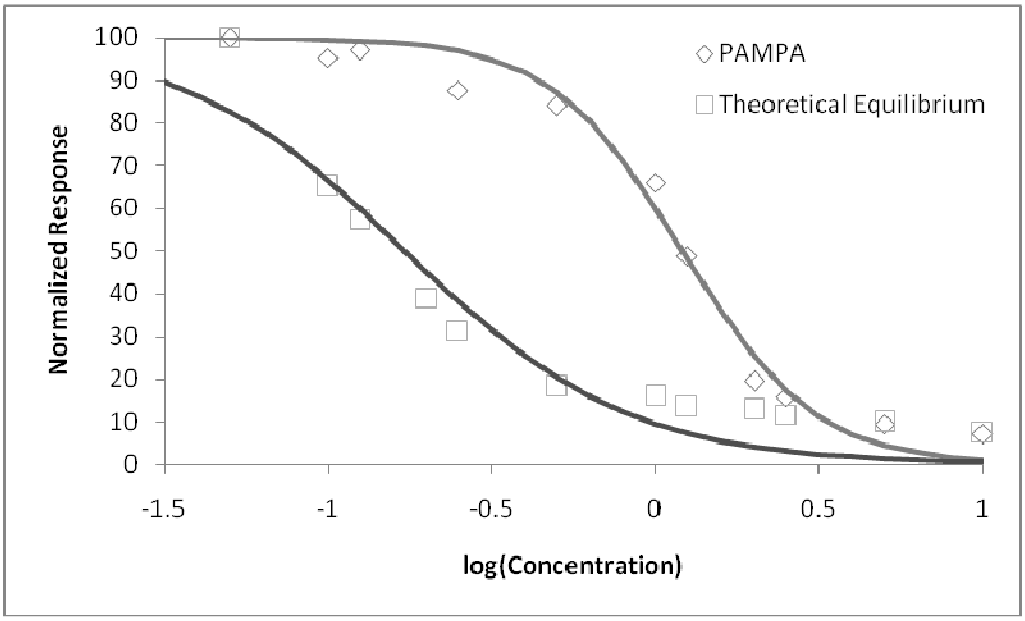

Figure 2-5 Dose response curves for ketoconazole

2.3.5 Permeability and the time response of ketoconazole

In order to maintain the high-throughput application of PAMPA, a reduction is assay time would be advantageous. Figure 2-6 shows the effect of the PAMPA incubation time on the apparent permeability on three known inhibitors of CYP3A4. Ketoconzole and verapamil were selected due to their relatively low and high permeability, respectively. Erythromycin was also analyzed in order to examine if variations in incubation time could explain the variable permeability values found in literature.

The solid lines in Figure 2-6 correspond to the percent inhibition caused by the compound in the acceptor well and the dashed lines represent the apparent permeability. The minimum incubation time is dependent on the compound with the lowest permeability; ketoconazole reaches the minimum required concentration after approximately 6 h. Verapamil initially exhibits very high permeability and approaches equilibrium between the wells after approximately 4 h. At 12 h, the amount of verapamil in the acceptor well is equal to the theoretical equilibrium concentration which prevents calculation of permeability due to the limitations of equation 3. Erythromycin demonstrates a strong time-dependency on permeability which could explain the large variability in reported literature values. Based on the results from these three compounds, the PAMPA incubation time could be reduced to 8 h. More compounds should be tested that cover a range of inhibitor strength and permeability before the assay time can be reduced further.

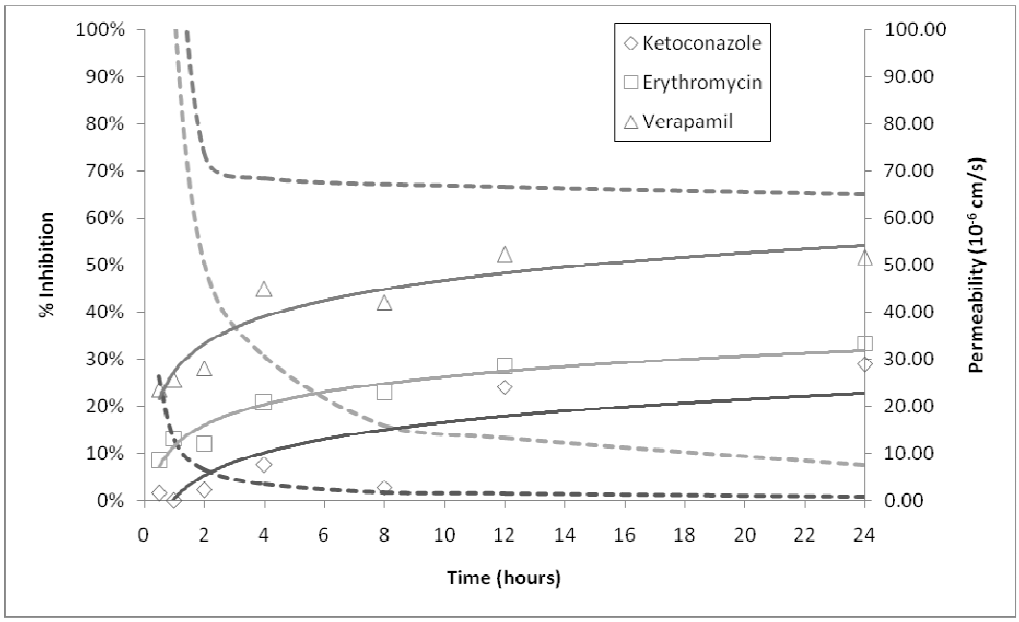

Figure 2-6 Effect of PAMPA incubation time on the calculated permeability and percent inhibition of ketoconazole

2.4 Conclusions

By multiplexing PAMPA with a fluorescence-based CYP inhibition assay, a new method amenable to automation has been developed to assess compound permeability in the early stages of drug development. This approach overcomes some of the limitations of traditional PAMPA including compound insolubility at high concentrations and detection of compounds lacking a suitable chromophore. Additionally, the increased sensitivity cuts the overall assay time in half as low permeability compounds can be detected at lower concentrations. The sensitivity of the fluorescence assay allows PAMPA to be run at physiologically-relevant doses, thus providing more accurate assessment of *in vivo* permeability.

In addition to permeability data, the addition of an inhibition assay as detection method provides supplementary information. For compounds with unknown IC_{50} values, the combined assay could be performed at a single high concentration which would allow for identification of drugs that are non-inhibitors or that have a limited effect due to poor permeability as well as drugs that strongly inhibit CYPs. If a permeability value is still desired for compounds at the two extremes of the inhibition curve, then the concentration can be adjusted accordingly and the assay repeated.

Figure 2-7 is a flow chart for use of the PAMPA/inhibition assay. The most straightforward case is measuring permeability for compounds with known IC_{50} values as this can be done in one step. If the primary intent is to screen unknown compounds for CYP inhibition, while taking into account the effect of permeability, then all compounds should be screened at a concentration threshold above which any CYP

inhibition would not be considered therapeutically relevant. Compounds that exhibit no inhibition in the PAMPA wells, as well as their corresponding theoretical equilibrium, can be discarded as non-inhibitors. For compounds with unknown IC_{50} values, an inhibition assay can be independently performed, or all compounds can be screened at a starting concentration of 5 μM. If the resulting inhibition lies outside the 10-90% range, the concentration is adjusted accordingly and the assay repeated. The process then becomes iterative, depending on the level of information needed. If the objective is to broadly classify compounds as inhibitors/non-inhibitors and low/medium/high permeability, then one to two iterations of the PAMPA/inhibition assay should be sufficient.

Multiplexed assays, such as the PAMPA/inhibition method, have the potential to be very powerful tools throughout the early drug discovery process. At the earliest stages, these types of assays can eliminate compounds with poor pharmacokinetic or ADME/Tox properties more quickly than performing individual assays. Here, we also observe that by subsequently performing an inhibition assay, permeability can be measured for compounds that could not be analyzed by traditional PAMPA due to lack of a suitable chromophore. Therefore, permeability can be measured for *all* compounds that inhibit various CYPs at clinical doses as opposed to the high concentrations required by traditional UV/Vis detection.

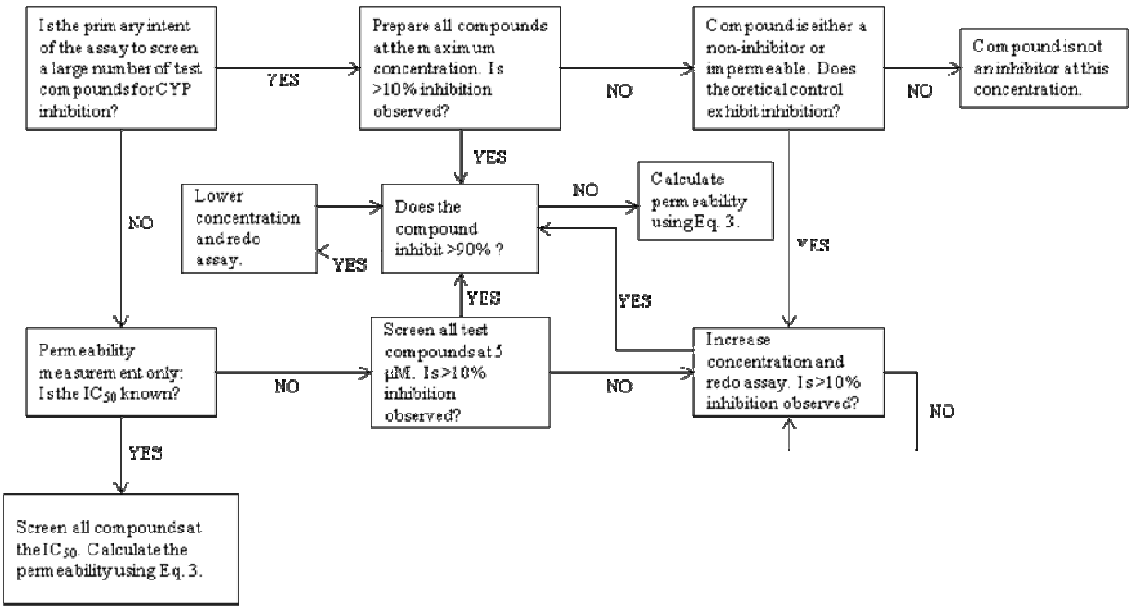

Figure 2-7 Flow chart for use of the PAMPA/inhibition assay

3. Fluorescence Reporter Gene Assay for CYP1A1 Induction

3.1 Introduction

The broad substrate specificity of CYPs can be problematic as inhibition and induction of CYPs by a large variety of compounds may result in drug-drug interactions (DDIs) (Cupp, 1998). Inhibition results in a decrease in CYP activity, therefore increasing the potential for a toxic build-up of a compound in the body. CYP induction results in an increase in CYP production and therefore an increase in CYP activity. If one compound increases the activity of a CYP that metabolizes a second compound, the overall effect of the second drug can have two effects (Whitlock, 1999). If the drug is metabolized into an inactive form, induction can result in an undesired loss of efficacy. On the other hand, if the drug is metabolized into its active form, a sudden spike in concentration can lead to a toxic event. A classic example of an induction-based DDI is the combination of fluconazole (Diflucan®) and warfarin (Coumadin®). Fluconazole is a common anti-fungal drug that strongly induces CYP2C9 and warfarin is an anti-coagulant. Patients taking warfarin concurrently with fluconzole have trouble achieving therapeutic levels of the anti-coagulant because it is actively metabolized by CYP2C9.

Many high-throughput *in vitro* assays are currently used to measure CYP inhibition, which employ the use of a spectroscopic technique (mass spectrometry) or a reporter substrate (fluorescence, luminescence, radioactivity). CYP induction involves a complex pathway that is isoform-specific. For this reason, assays developed to measure CYP induction tend to be based upon whole-cell models (Soars, 2007; Vermeir, 2005). Primary human hepatocytes have been recognized as the gold standard for CYP

induction studies and are the preferred method recognized by the FDA. The major drawbacks of primary hepatocytes include high cost, high variability, and loss of activity in suspension after relatively short periods of time. Alternatives to primary hepatocytes include cyropreserved hepatocytes (Kafert-Kasting, 2006), liver slices, recombinant expression models, and immortalized cell lines. Immortalized cell lines have the major advantage of unlimited proliferation, but the use of this approach has been limited by the inability to significantly induce expression of CYPs. More recently, the development of cell lines capable of higher CYP expression upon induction has been reported (Youdim, 2007; Mills, 2004; Noracharttiyapot, 2006). Another attractive method is the development of reporter cell line induction assays. A construct consisting of a reporter gene and specific segments of the induction elements from a CYP gene are transfected into a suitable human-derived (HepG2) or animal-derived cell line, such as rat-derived H4IIE cells. These assays are amenable to high-throughput platforms and appear to be a suitable option for early prediction of *in vivo* induction profiles. The past ten years have shown increased use of luciferase reporter assays (Cui, 2002; Werlinder, 2001). One of the major drawbacks of luciferase is that the cells must be lysed in order to run the assay. This not only reduces the throughput of the assay, but also prohibits monitoring gene expression after induction unless additional samples are prepared. An alternative to luciferase is green fluorescent protein (GFP), which can be directly assayed using a standard fluorescent plate reader or microscope (Operana, 2007; Zhao, 2004).

Other methods used to measure CYP induction include northern blot analysis, western blot analysis, the electrophoretic mobility shift assay (EMSA), the ethoxyresorufin-*O*-dealkylation (EROD) activity assay, and qualitative real-time RT-

PCR. While many of these methods are used to validate new induction assays, they tend to be low-throughput and labor intensive.

CYP1A1 induction is one of the most well-studied and well-understood among all of the CYP induction pathways (see Figure 3-2). The main group of compounds associated with CYP1A1 induction is the polycyclic aromatic hydrocarbons (PAHs), which have the interesting capability of inducing their own metabolism (Whitlock, 1999). The PAHs ultimately form a complex with the two major proteins involved in the CYP1A1 induction pathway; the aryl hydrocarbon receptor (AhR) binds the inducer and the Ah receptor nuclear translocator (Arnt) dimerizes with the AhR complex in the nucleus. These proteins are always present in the cell and therefore induction can occur quickly in absence of a protein synthesis requirement. 2,3,7,8-Tetrachlorodibenzo-*p*-dioxin (TCDD), an environmental toxin, is an extremely potent inducer of CYP1A1 and has traditionally played a major role in CYP1A1 induction research. Studies focusing on the mechanism of TCDD-mediated induction have played a large role in explaining the relationship between certain genetic polymorphisms and susceptibility to cancer. The extreme potency of TCDD restricts its use in some research labs and alternatives must be used. Other compounds that are suitable inducers of CYP1A1 include 7,12-dimethylbenzanthracene (DMBA), α and β-naphthoflavone (αNF and βNF), and 3-methylcholanthrene (Cui, 2002). Indole-3-carbinol (I3C) is a weak inducer and can be used to validate the detection capability of new assays. The structures of these compounds are shown in Figure 3-1.

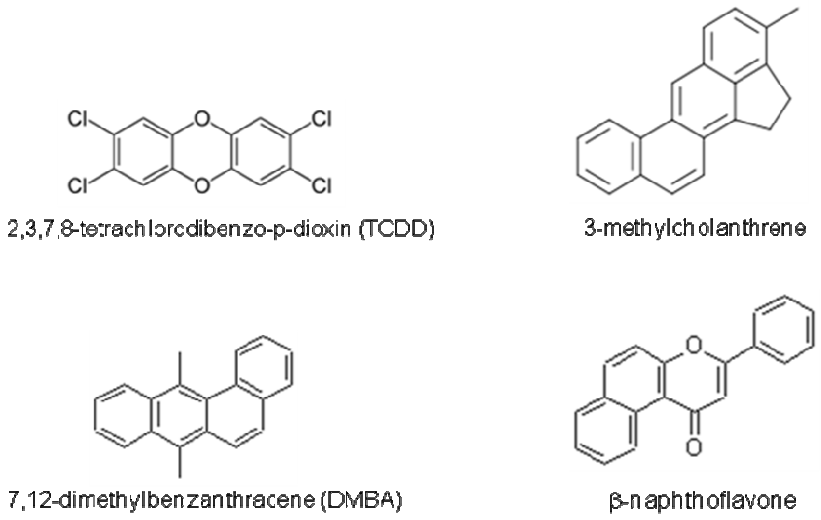

Figure 3-1 Known inhibitors of CYP1A1

The mechanism for CYP1A1 induction is shown in Figure 3-2. The receptive configuration of AhR is maintained by the 90 kDa heat shock protein (hsp90) and AhR-interacting protein (AIP) until an inducer binds. Hsp90 and AhR dissociate and the AhR-ligand complex undergoes nuclear translocation. The AhR complex then dimerizes with Arnt and can bind to the enhancer, which is rich in xenobiotic response elements (XREs). Transactivation domains of AhR interact with transcription elements that bind to the promoter. An initiation complex forms and transcription can begin. It is important to note that the promoter is silent in absence of enhancer binding. A summary of the other major pathways is shown in Figure 3-3. Complications arise when considering some of the more important CYPs such as CYP3A4 and CYP2C9 due to cross-talk between pathways (Waxman, 1999).

H4IIE, a rat hepatoma cell line, was selected for use as a model system because CYP1A1 is highly inducible, has low basal CYP1A1 activity, and exhibits good growth characteristics. The FDA has used H4IIE cells in bioassays for environmental toxicant classification and detection of contaminants in food for over 25 years (Whyte, 2004). Human-derived hepatocellular carcinomas such as Hep3B and HepG2 were not used due to poor CYP1A1 inducibility. Lung-derived cell lines, such as A-427, could also be used as CYP1A1 is expressed at higher levels relative to other isoforms. Polymorphisms in the *CYP1A1* gene in lung tissue have been associated with smoking-induced lung cancer (Zhang, 2006).

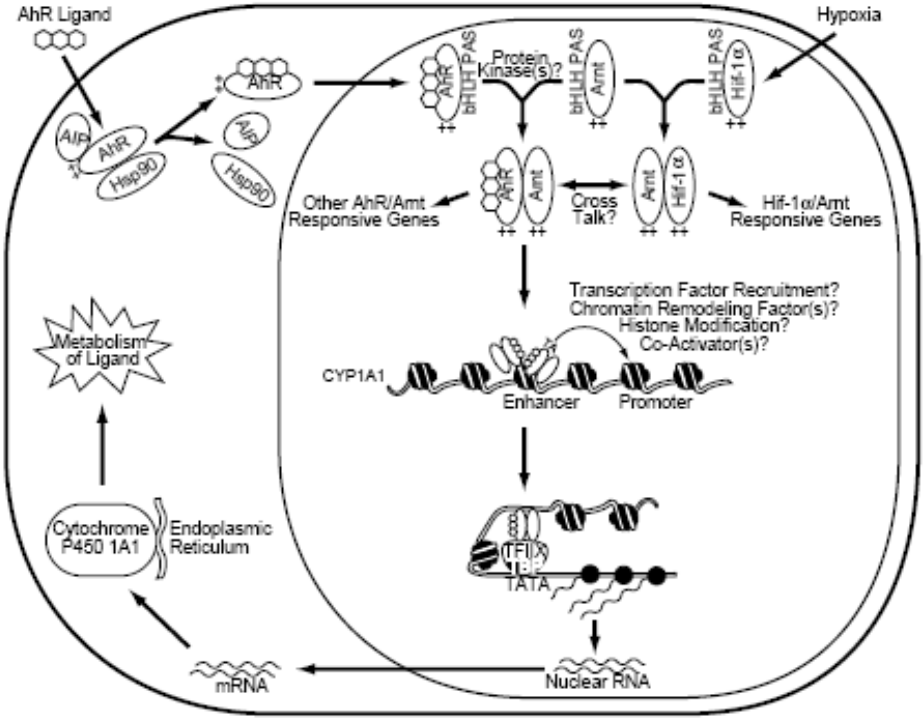

Figure 3-2 Induction mechanism of CYP1A1

(Whitlock, 1999)

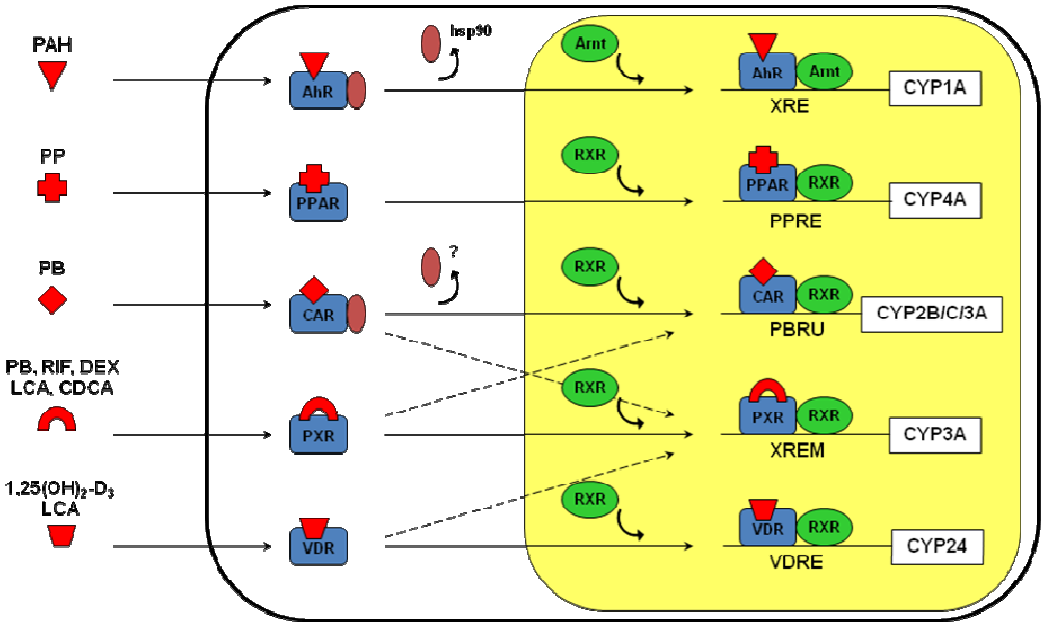

Figure 3-3 Induction pathways for several P450 isoforms

In this study, the development of a reporter gene assay for CYP1A1 induction is reported. Elements of the *CYP1A1* gene were inserted into a plasmid containing a destabilized variant of the GFP gene. The first approach was to insert a specific number of XREs and a promoter upstream of the GFP gene, transfect into H4IIE cells, and then measure fluorescence in response to an inducer. These constructs were then compared to those containing the 5'-flanking region of the *CYP1A1* gene with its native promoter. The effect of inserting a stronger promoter in addition to the *CYP1A1* gene was also examined. The goal of this project is to develop a reporter cell line capable of measuring the potential of a compound to induce CYP1A1, which will ultimately be amenable to adaption to a microarray platform.

3.2 Materials and Methods

3.2.1 Materials

α-Naphthoflavone (αNF), kanamycin, and cell-culture grade DMSO were purchased from Sigma (St. Louis, MO). Restriction and other DNA-modifying enzymes were obtained from New England BioLabs (Ipswich, MA). H4IIE cells, cell culture media, and fetal bovine serum (FBS) were purchased from ATCC (Manassas, VA). PCR primers were purchased from IDT (Coralville, IA). All other PCR products were obtained from Promega (Madison, WI). DNA and gel purification kits were purchased from Qiagen (Valencia, CA). Any additional culture reagents and molecular cloning materials were obtained from Invitrogen (Carlsbad, CA).

3.2.2 Instrumentation

DNA concentrations were measured using a NanoDrop ND-1000 spectrophotometer (NanoDrop Technologies, Wilmington, DE). All fluorescence microscopy was performed with a Nikon Eclipse TS100 microscope (Nikon USA, Melville, NY) using a EXFO X-Cite 120 fluorescence illumination system (EXFO, Quebec, Canada). Fluorescence measurements were made with a Perkin Elmer HTS 7000 Bio Assay plate reader (Perkin Elmer, Waltham, MA).

3.2.3 Reporter gene constructs

A 3X-XRE sequence (5'-AATTCGAGCTCGGAGTTGCGTGAGAAGAGCC GAGCTCGGAGTTGCGTGAGAAGAGCCGAGCTCGGAGTTGCGTGAGAAGAGC CG-3' and 5'-AATTCGGCTCTTCTCACGCAACTCCGAGCTCGGCTCTTCTCAC GCAACTCCGAGCTCGGCTCTTCTCACGCAACTCCGAGCTCG-3') was designed with *Eco*R I restriction sites at both ends (Backlund, 1997). A minimum promoter element (5'-CAGAGGGTATATAATGGAAGCTCGACTTCCAGG-3' and 5'-GATCC CTGGAAGTCGAGCTTCCATTATATACCCTCTGGTAC-3') was also made with *Kpn* I and *Bam*H I sites at the 5' and 3' ends, respectively. The complimentary sequences were annealed and then phosphorylated in order to increase ligation efficiency. The pZsGreen1-DR vector (Clontech, Mountain View, CA) was digested with the appropriate restriction enzyme(s), dephosphorylated, and gel purified with a QIAquick Gel Extraction Kit (Qiagen) before the enhancer or promoter element was inserted. After each ligation, the presence of the insert was confirmed by restriction mapping. For the minimum promoter, the insert replaces a segment in the multiple

cloning site (MCS) that contains the restriction site *Apa* I. Therefore digestion with this enzyme will not cut the vector if the minimum promoter has been correctly incorporated. The final construct was named XRE-minPmo-pZsGreen1.

A second set of reporter gene constructs were made by replacing the minimum promoter with the SV40 promoter from the pGL3-Promoter vector (Promega). The 202 bp SV40 promoter was amplified using the primer pair SV40PmoF (5'-GTTGTTGGTACCTGCATCTCAATTAGTCAGCAACC-3') and SV40PmoR (5'-GTTGTTGGATCCAAGCTTTTTGCAAAAGCCTAGG-3'). The restriction sites for *Kpn* I and *Bam*H I were engineered into the forward and reverse primers, respectively. The PCR product was digested with the appropriate restriction enzymes and gel purified. The minimum promoter was removed from the XRE-minPmo-pZsGreen1 vector and replaced with the purified PCR product. This construct is referred to as XRE-SV40-pZsGreen1.

The final set of constructs contained a 1212 bp region of the rat CYP1A1 5'-flanking region. This segment was amplified from rat genomic DNA (Clontech) using the PCR primer pair 5'FlankCYP1A1F (5'-GTTGTTAGATCTCTGGCGCTGTCTAG TCGC-3') and 5'FlankCYP1A1R (5'-GTTGTTGAATTCGGTTAGGGTGAAGGCAC CA-3'). The amplified region starts at the position -1213 and continues to -1 relative to the CYP1A1 start site. The restriction sites for *Bgl* II and *Eco*R I were added to the forward and reverse primers, respectively. After digesting the PCR product and the pZsGreen1-DR vector with the appropriate restriction enzymes, the amplified 5'-flanking region was inserted via ligation into the purified vector. Presence of the insert was confirmed by restriction mapping. Once again, the insert replaces a segment in the

MCS that contains the restriction site *Sac* I. If the insert is present then treatment with *Sac* I will not cut the plasmid. The final construct was named 5'FlankCYP1A1-pZsGreen1. An additional construct called 5'FlankCYP1A1-SV40-pZsGreen1 was made by removing the XRE from XRE-SV40-pZsGreen1 and inserting the flanking region upstream of the additional SV40 promoter.

For all constructs, larger DNA preparations were made using DH5α chemically competent *E. coli* (Invitrogen). The DNA was purified using either a QIAprep Spin Miniprep Kit or a HiSpeed Plasmid Midi Kit (Qiagen). The final concentration and purity of each plasmid was determined using the NanoDrop instrument.

3.2.4 Cell culture and transient transfection

The rat hepatoma cell line H4IIE was cultured in Eagle's Minimum Essential Medium (EMEM) supplemented with 10% FBS at 37°C and 5% CO_2. Twenty-four hours prior to transfection, a tissue culture flask containing cells at no greater than 80% confluence was used to seed a 24-well tissue culture plate at a density of $5x10^4$ cells/mL ($2.5x10^4$ cells/well). The appropriate plasmid (0.3 μg/well) was transfected with Lipofectamine (Invitrogen) in a serum-free, antibiotic-free environment according to the manufacturer's instructions. pZsGreen1-DR was used as a negative control (no enhancer or promoter) and a plasmid that constitutively expresses GFP under control of the CMV promoter was used as a positive control. Additional controls were also prepared to account for any induction by DMSO. After 3 h, medium containing 2X serum was added to the cells. The positive control wells were checked for GFP activity

under a fluorescence microscope 24 h after transfection. If expression was present, the cells were then treated with varying concentrations (1-30 μM) of αNF in DMSO.

3.2.5 Fluorescence microscopy and spectroscopy

The induced cells were checked for gene expression after 24, 48, and 72 h using a fluorescence microscope containing a GFP filter set. If high background was observed after 72 h due to phenol red interference, the medium was carefully replaced with an equal volume of PBS (pH 7.4). The 24-well plates were all scanned in a fluorescence plate reader using an excitation wavelength of 485 nm and an emission wavelength of 535 nm.

3.3 Results and Discussion

3.3.1 Analysis of the reporter gene constructs

Restriction mapping of the XRE-minPmo-pZsGreen1 constructs confirmed the presence of both the XRE and minimum promoter inserts. However, one of the selected constructs appeared to contain two copies of the XRE element. DNA sequencing confirmed this hypothesis, and the two constructs were renamed 3X-XRE-minPmo-pZsGreen1 and 6X-XRE-minPmo-pZsGreen1. It was additionally found that several constructs had incorporated the XRE sequence backwards due to the use of *Eco*R I at both ends of the insertion sequence. This should not impact the role of the enhancer element as it has been previously shown that the effect of the enhancer is independent of the orientation (Sogawa, 1986).

The consensus sequence for the XRE is 5'-(G/C)N(T/G)(A/G)GCTGGG-3' in rat CYP1A1. Figure 3-4 shows the PCR amplified region of the 5'-flanking region of the rat *CYP1A1* gene. This region contains seven XREs upstream of the promoter region as well as several negative regulatory sequences. The inserts for the 5'-flanking region and the SV40 promoter contain unique restriction sites on either end in order to ensure proper orientation.

Figure 3-4 5'-flanking region of the *CYP1A1* gene

Bold, italicized – XRE elements

Underlined – Restriction sites

Bold – Promoter site (TATA box)

(Sogawa, 1986)

3.3.2 3X/6X-XRE-minPmo-pZsGreen1

The first set of constructs tested were the plasmids containing 3X or 6X-XREs and the minimum promoter. The minimalist approach used to design these constructs asks two important questions: 1) In the absence of the native promoter, will the XREs be enough to initiate expression of GFP? 2) Will the minimum promoter be strong enough drive GFP expression when induced and more importantly, because it is not the native promoter, is the basal expression of GFP low?

Initially, cells were treated with either 10 μM αNF, 30 μM αNF, or an equal volume of DMSO. No significant fluorescence was observed after 24 h with the exception of the positive control. After 48 h, some gene expression is observed, but not at significant levels over the background fluorescence. Figure 3-5 contains images taken after 72 h of incubation. While some fluorescence is observed, the level of fluorescence does not seem to vary between the DMSO-treated wells versus the αNF-treated wells. Additionally, no difference is observed between cells transfected with 3X-XRE-minPmo-pZsGreen1 versus 6X-XRE-minPmo-pZsGreen1.

Because no significant increase in GFP expression is observed in the presence of αNF over the DMSO controls, it is implied that the minimal promoter does not interact with the enhancer elements strongly enough to see a concentration-dependent induction effect. Some isolated cells containing the 6X-XRE-minPmo-pZsGreen1 treated with 30 μM inducer did exhibit gene expression, but these events were rare and inconsistent. While the basal level of GFP expression was indeed low, a stronger promoter is needed in order to see a measurable amount of gene activation and expression.

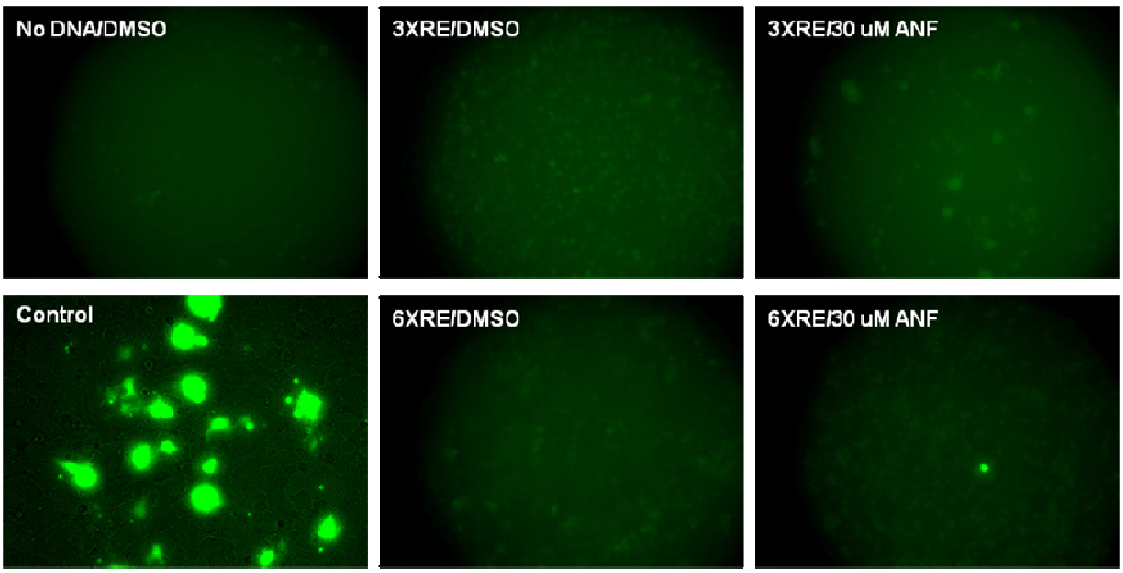

Figure 3-5 Fluorescence microscopy of induced H4IIE cells

3.3.3 5'-FlankCYP1A1-pZsGreen1

Constructs similar to 5'FlankCYP1A1-pZsGreen1have been previously reported in literature, but differ in respect to the use of luciferase instead of GFP. Because this construct will contain both positive and negative regulatory sequences as well as the native promoter for the *CYP1A1* gene, the induction potential of other constructs can be compared to this more "native" reporter gene construct. The segment of the 5'-flanking region inserted into the reporter vector has been shown to exhibit a 12-fold induction by 3-methylcholanthrene as compared to 21-fold induction when the gene is left intact. The XREs critical to induction are contained within the 1212 bp segment insert used to in these reporter gene constructs. Additionally, the same study demonstrated that XREs could act upon heterologous promoters and the effect is relatively independent of distance from the promoter and enhancer orientation. The induction response of 5'FlankCYP1A1-pZsGreen should be comparable to results previously reported in literature and will therefore serve as a benchmark for comparison.

3.3.4 Addition of the SV40 promoter

The SV40 promoter was inserted in place of the minimum promoter in 3X/6X-XRE-minPmo-pZsGreen1 and after the 5'-flanking segment in 5'FlankCYP1A1-pZsGreen1. The promoter element must be strong enough to drive measurable expression of GFP, but have low enough background fluorescence from constitutive expression to avoid masking the effect of induction. The SV40 (simian vacuolating virus 40) promoter is stronger than the minimal promoter as more transcription factors (TFs) are known to bind to it, but is less promiscuous than the CMV (cytomegalovirus)

promoter. A comparison of promoter length suggests that that the 30 bp minimal promoter contains less TF binding sequences than the 200 bp SV40 promoter, which would subsequently have less TF binding sites than the 550 bp CMV promoter.

3.3.5 Comparison of constructs

3X/6X-XRE-SV40-pZsGreen1, 5'FlankCYP1A1-pZsGreen1, and 5'FlankCYP1A1-SV40-pZsGreen1 were induced with 1, 3, 10, and 30 μM αNF. Fluorescence microscopy and plate reader measurements did not indicate significant gene expression at 24 and 48 hours. After 72 hours, gene expression was observed and a comparison of the constructs is shown in Figure 3-6. The fluorescence of the DMSO control for each construct is subtracted out from the corresponding αNF-induced wells. Images obtained from the fluorescence microscope for several constructs are shown in Figure 5-7. The number of XREs present in the construct did not appear to have a major impact on the expression of GFP, so the 6X-XRE construct was selected for further use as it gives more consistent results. This is presumably due to an increase in the number of binding sites available for the AhR/Arnt complex.

From Figure 3-6, it appears that the 5'FlankCYP1A1-SV40-pZsGreen1 construct is most significantly induced by αNF at high concentrations followed by the 6X-XRE and 5'FlankCYP1A1 which exhibit comparable induction response. As the concentration of αNF decreases, the response of 6X-XRE-SV40-pZsGreen1 exhibits the most gradual decline. The constructs that contain the 5'-flanking region of the *CYP1A1* gene exhibit a significant difference, which is presumably due to transcription factors having a higher binding affinity for the SV40 promoter. The same reasoning applies to

the 6X-XRE construct. The lack of competing promoter may allow for higher consitutive expression at lower concentrations. Comparing the dose-response results obtained here with reporter gene constructs that use luciferase (Cui, 2002), comperable profiles are observed.

Comparison of the three constructs in Figure 3-6 suggests that either of the 5'FlankCYP1A1 constructs would be suitable for use in further assay development. Both constructs exhibit a steeper dose-response curve than the 6X-XRE construct. In other words, the exposure to an inducer appears to exhibit a more dramatic response and will have a higher calculated fold-of-induction. The use of 5'FlankCYP1A1-SV40-pZsGreen1 may have be advantageous in situations where detection sensitivity is an issue (e.g. low cell numbers, low induction effects).

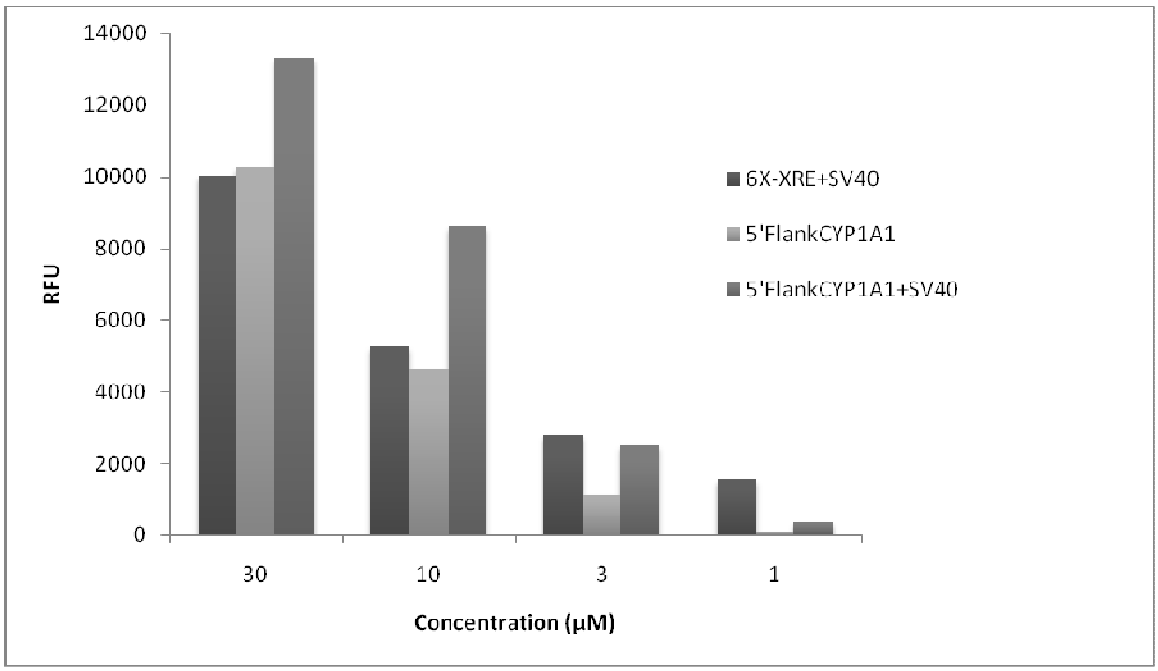

Figure 3-6 Comparison of reporter gene constructs induced with various concentrations of αNF

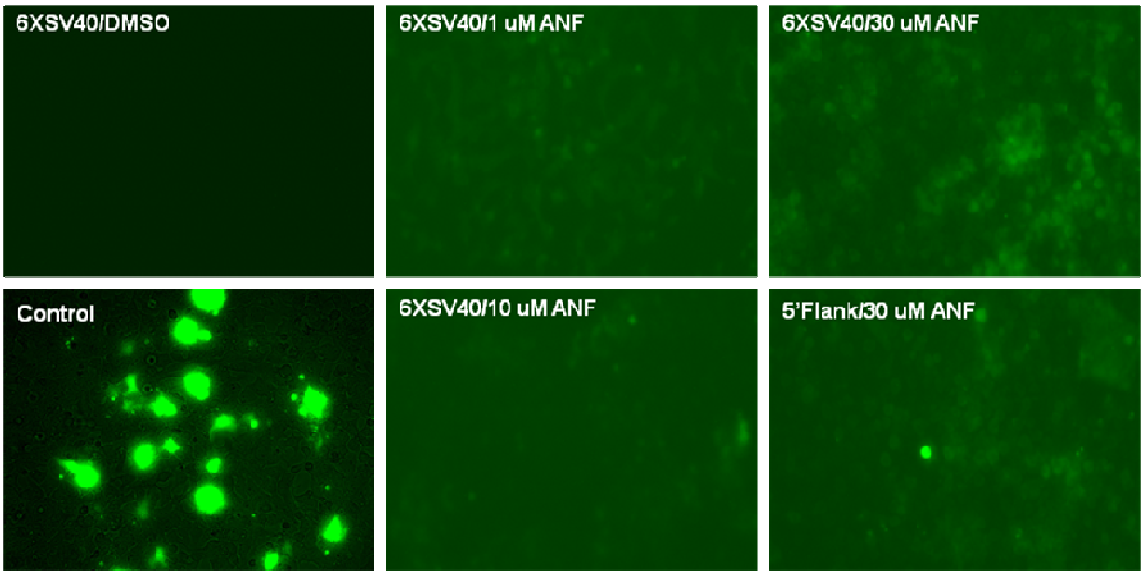

Figure 3-7 Microscope images of transfected H4IIE cells induced with αNF

3.3.6 Assay improvements and future work

One major problem with the assay is that phenol red, which is used in the media as a pH indicator, exhibits high background fluorescence. Replacing the media with PBS before plate reader measurements can significantly reduce the background, but cells are easily sloughed away resulting in measurement error. Additionally, this process would have to be repeated at every time point a measurement is required. This suggests that a phenol red-free medium comparable to the normal growth medium should be used for all fluorescence measurements.

Ultimately, it is desirable to adapt this induction assay to a microarray format similar to the work published by Lee *et al.* (Lee, 2008). The small volumes used for each spot in these microarrays can only accommodate a limited number of cells. Transfection effeciency must be optimized in order to ensure that each spot has plasmid-containing cells. In addition to optimizing the transfection process, dual reporter vectors could be made which would allow for visualization of transfection therefore eliminating the need for cotransfection as a control. In Figure 3-8 a second reporter gene such as red fluorescent protein (RFP) is added in under constitutive expression of the CMV promoter. All cells that successfully uptake the plasmid will express RFP which can be visualized using a scanner. Upon induction, these same cells should begin to produce GFP which can be visualized using a different filter set. The images could then be superimposed to see the overall impact of induction similar to some cell viability assays. An overall schematic of the proposed microarray format is shown in Figure 3-9

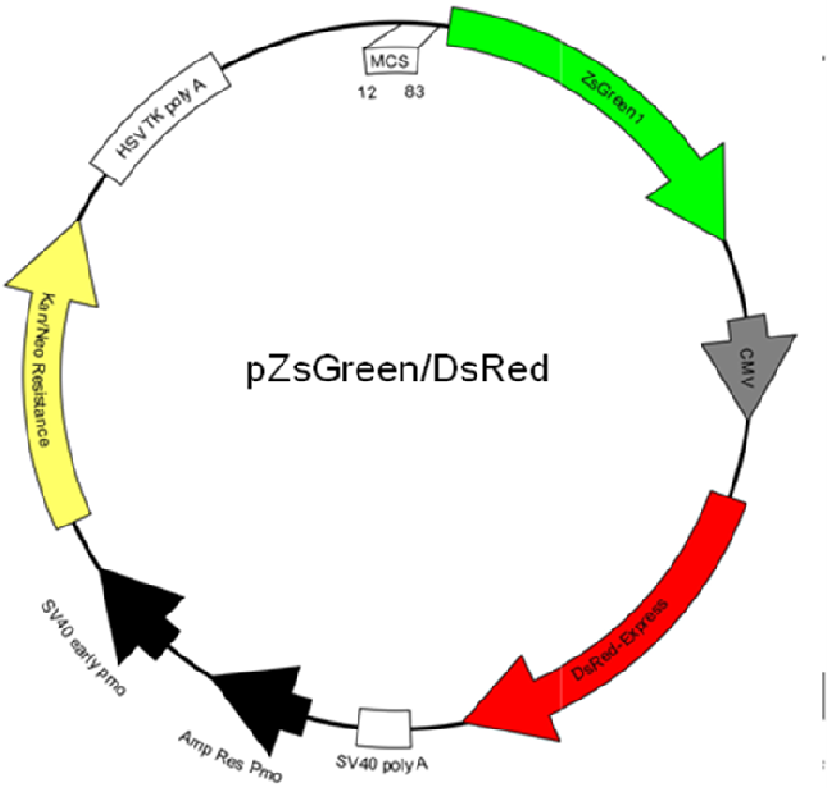

Figure 3-8 Proposed dual reporter vector for measurement of CYP induction

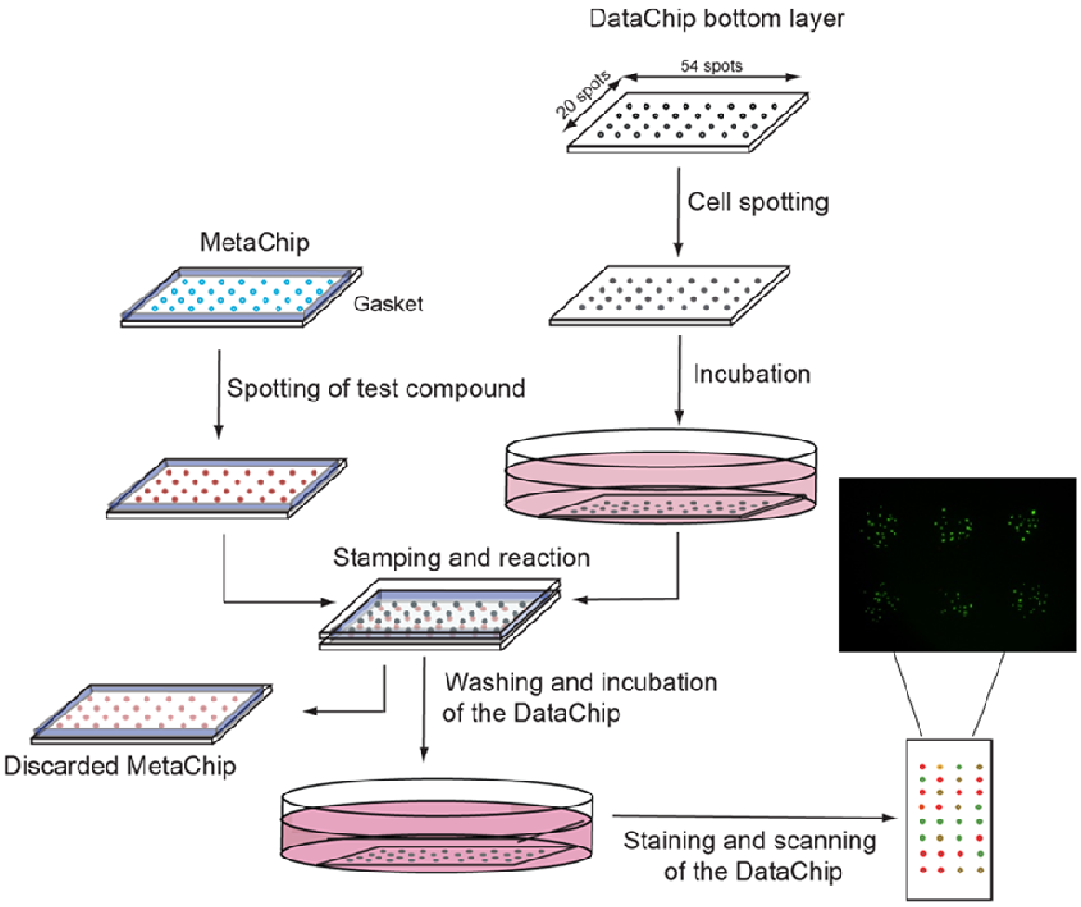

Figure 3-9 Schematic of the proposed induction microarray

3.4 Conclusions

In this study, six different reporter gene constructs were created to measure the induction of CYP1A1. The influence of the number of XREs and promoter strength on induction was initially the main focus. It was determined that the number of XRE elements does not have a significant role on the amount of gene expression, but results are more consistent as the number of XREs in the enhancer increases. αNF was used as a prototypical inducer of CYP1A1, and a dose response similar to previously published results using a luciferase assay was obtained. The promoter strength had an effect on the basal level of GFP expression. When only the native CYP1A1 promoter was present, almost no constitutive GFP expression was observed, whereas the minimum promoter and SV40 both exhibited background expression. The native and SV40 promoters were both inducible, but the minimum promoter was not.

Recommendations for future assay development include the optimization of a phenol red-free media to reduce background fluorescence, optimization of transfection efficiency, and the incorporation of a second consititutively expressed fluorescent protein for use a transfection marker. Either of the constructs containing the 5'-flanking region would be suitable for future use. The construct containing the additional SV40 promoter has a higher overall expression of GFP and will therefore have a slight advantage if sensitivity is an issue.

4. References

Al-Dosari, M., G. Zhang, et al. (2006). "Direct assessment of promoter activity of human cytochrome p450 genes using optimized transfection in vitro and in vivo." Biosci Rep **26**(3): 217-29.

Avdeef, A. (2005). "The rise of PAMPA." Expert Opin Drug Metab Toxicol **1**(2): 325-42.

Avdeef, A., P. Artursson, et al. (2005). "Caco-2 permeability of weakly basic drugs predicted with the double-sink PAMPA pKa(flux) method." Eur J Pharm Sci **24**(4): 333-49.

Avdeef, A., S. Bendels, et al. (2007). "PAMPA--critical factors for better predictions of absorption." J Pharm Sci **96**(11): 2893-909.

Avdeef, A., P. E. Nielsen, et al. (2004). "PAMPA--a drug absorption in vitro model 11. Matching the in vivo unstirred water layer thickness by individual-well stirring in microtitre plates." Eur J Pharm Sci **22**(5): 365-74.

Backlund, M., I. Johansson, et al. (1997). "Signal transduction-mediated activation of the aryl hydrocarbon receptor in rat hepatoma H4IIE cells." J Biol Chem **272**(50): 31755-63.

Balimane, P. V., E. Pace, et al. (2005). "A novel high-throughput automated chip-based nanoelectrospray tandem mass spectrometric method for PAMPA sample analysis." J Pharm Biomed Anal **39**(1-2): 8-16.

Bessette, E. E., M. J. Fasco, et al. (2005). "Mechanisms of arsenite-mediated decreases in benzo[k]fluoranthene-induced human cytochrome P4501A1 levels in HepG2 cells." Drug Metab Dispos **33**(3): 312-20.

Chefson, A. and K. Auclair (2006). "Progress towards the easier use of P450 enzymes." Mol Biosyst **2**(10): 462-9.

Cui, X., J. Palamanda, et al. (2002). "A high-throughput cell-based reporter gene system for measurement of CYP1A1 induction." J Pharmacol Toxicol Methods **47**(3): 143-51.

Cupp, M. J. and T. S. Tracy (1998). "Cytochrome P450: new nomenclature and clinical implications." Am Fam Physician **57**(1): 107-16.

DeWitte, R. S. (2006). "Avoiding physicochemical artefacts in early ADME-Tox experiments." Drug Discov Today **11**(17-18): 855-9.

Di, L., E. H. Kerns, et al. (2003). "High throughput artificial membrane permeability assay for blood-brain barrier." Eur J Med Chem **38**(3): 223-32.

Di, L., E. H. Kerns, et al. (2007). "Comparison of cytochrome P450 inhibition assays for drug discovery using human liver microsomes with LC-MS, rhCYP450 isozymes with fluorescence, and double cocktail with LC-MS." Int J Pharm **335**(1-2): 1-11.

Dierks, E. A., K. R. Stams, et al. (2001). "A method for the simultaneous evaluation of the activities of seven major human drug-metabolizing cytochrome P450s using an in vitro cocktail of probe substrates and fast gradient liquid chromatography tandem mass spectrometry." Drug Metab Dispos **29**(1): 23-9.

Flaten, G. E., A. B. Dhanikula, et al. (2006). "Drug permeability across a phospholipid vesicle based barrier: a novel approach for studying passive diffusion." Eur J Pharm Sci **27**(1): 80-90.

Galinis-Luciani, D., L. Nguyen, et al. (2007). "Is PAMPA a useful tool for discovery?" J Pharm Sci **96**(11): 2886-92.

Gozgit, J. M., K. M. Nestor, et al. (2004). "Differential action of polycyclic aromatic hydrocarbons on endogenous estrogen-responsive genes and on a transfected estrogen-responsive reporter in MCF-7 cells." Toxicol Appl Pharmacol **196**(1): 58-67.

Hidalgo, I. J. (2001). "Assessing the absorption of new pharmaceuticals." Curr Top Med Chem **1**(5): 385-401.

Hughes, B. (2008). "2007 FDA drug approvals: a year of flux." Nat Rev Drug Discov **7**(2): 107-9.

Hunt, L., M. Jordan, et al. (1999). "GFP-expressing mammalian cells for fast, sensitive, noninvasive cell growth assessment in a kinetic mode." Biotechnol Bioeng **65**(2): 201-5.

Ingels, F. M. and P. F. Augustijns (2003). "Biological, pharmaceutical, and analytical considerations with respect to the transport media used in the absorption screening system, Caco-2." J Pharm Sci **92**(8): 1545-58.

Kafert-Kasting, S., K. Alexandrova, et al. (2006). "Enzyme induction in cryopreserved human hepatocyte cultures." Toxicology **220**(2-3): 117-25.

Kansy, M., A. Avdeef, et al. (2004). "Advances in screening for membrane permeability: high-resolution PAMPA for medicinal chemists." Drug Discov Today: Tech **1**(4): 349-55.

Kansy, M., F. Senner, et al. (1998). "Physicochemical high throughput screening: parallel artificial membrane permeation assay in the description of passive absorption processes." J Med Chem **41**(7): 1007-10.

Kariv, I., R. A. Rourick, et al. (2002). "Improvement of "hit-to-lead" optimization by

integration of in vitro HTS experimental models for early determination of pharmacokinetic properties." Comb Chem High Throughput Screen **5**(6): 459-72.

Kassel, D. B. (2004). "Applications of high-throughput ADME in drug discovery." Curr Opin Chem Biol **8**(3): 339-45.

Kerns, E. H. and L. Di (2003). "Pharmaceutical profiling in drug discovery." Drug Discov Today **8**(7): 316-23.

Kerns, E. H., L. Di, et al. (2004). "Combined application of parallel artificial membrane permeability assay and Caco-2 permeability assays in drug discovery." J Pharm Sci **93**(6): 1440-53.

Kumar, R. A. and D. S. Clark (2006). "High-throughput screening of biocatalytic activity: applications in drug discovery." Curr Opin Chem Biol **10**(2): 162-8.

Kumar, S., D. R. Davydov, et al. (2005). "Role of cytochrome B5 in modulating peroxide-supported cyp3a4 activity: evidence for a conformational transition and cytochrome P450 heterogeneity." Drug Metab Dispos **33**(8): 1131-6.

Lang, P., K. Yeow, et al. (2006). "Cellular imaging in drug discovery." Nat Rev Drug Discov **5**(4): 343-56.

Lee, M. Y., R. A. Kumar, et al. (2008). "Three-dimensional cellular microarray for high-throughput toxicology assays." Proc Natl Acad Sci U S A **105**(1): 59-63.

Lennernas, H. (1998). "Human intestinal permeability." J Pharm Sci **87**(4): 403-10.

Lentz, K. A., J. Hayashi, et al. (2000). "Development of a more rapid, reduced serum culture system for Caco-2 monolayers and application to the biopharmaceutics classification system." Int J Pharm **200**(1): 41-51.

Liang, E., K. Chessic, et al. (2000). "Evaluation of an accelerated Caco-2 cell

permeability model." J Pharm Sci **89**(3): 336-45.

McGee, P. (2005). "Tracking drug safety from the ground up." Drug Discovery and Development.

Mensch, J., M. Noppe, et al. (2007). "Novel generic UPLC/MS/MS method for high throughput analysis applied to permeability assessment in early Drug Discovery." J Chromatogr B Analyt Technol Biomed Life Sci **847**(2): 182-7.

Mills, J. B., K. A. Rose, et al. (2004). "Induction of drug metabolism enzymes and MDR1 using a novel human hepatocyte cell line." J Pharmacol Exp Ther **309**(1): 303-9.

Mohutsky, M. A., D. M. Petullo, et al. (2005). "The use of a substrate cassette strategy to improve the capacity and throughput of cytochrome P450 induction studies in human hepatocytes." Drug Metab Dispos **33**(7): 920-3.

Nicholson, R. L., M. Welch, et al. (2007). "Small-molecule screening: advances in microarraying and cell-imaging technologies." ACS Chem Biol **2**(1): 24-30.

Nielsen, P. E. and A. Avdeef (2004). "PAMPA--a drug absorption in vitro model 8. Apparent filter porosity and the unstirred water layer." Eur J Pharm Sci **22**(1): 33-41.

Noracharttiyapot, W., Y. Nagai, et al. (2006). "Construction of several human-derived stable cell lines displaying distinct profiles of CYP3A4 induction." Drug Metab Pharmacokinet **21**(2): 99-108.

O'Brien, S. E. and M. J. de Groot (2005). "Greater than the sum of its parts: combining models for useful ADMET prediction." J Med Chem **48**(4): 1287-91.

Omura, T. (2006). "Mitochondrial P450s." Chem Biol Interact **163**(1-2): 86-93.

Operana, T. N., N. Nguyen, et al. (2007). "Human CYP1A1GFP expression in transgenic mice serves as a biomarker for environmental toxicant exposure." Toxicol Sci **95**(1): 98-107.

Ortiz de Montellano, P. R. (1995). Cytochrome P450 : structure, mechanism, and biochemistry. New York, Plenum Press.

Ruell, J. A., K. L. Tsinman, et al. (2003). "PAMPA--a drug absorption in vitro model. 5. Unstirred water layer in iso-pH mapping assays and pKa(flux)--optimized design (pOD-PAMPA)." Eur J Pharm Sci **20**(4-5): 393-402.

Sambuy, Y., I. De Angelis, et al. (2005). "The Caco-2 cell line as a model of the intestinal barrier: influence of cell and culture-related factors on Caco-2 cell functional characteristics." Cell Biol Toxicol **21**(1): 1-26.

Seliskar, M. and D. Rozman (2007). "Mammalian cytochromes P450--importance of tissue specificity." Biochim Biophys Acta **1770**(3): 458-66.

Shah, P., V. Jogani, et al. (2006). "Role of Caco-2 cell monolayers in prediction of intestinal drug absorption." Biotechnol Prog **22**(1): 186-98.

Silva, J. M., P. E. Morin, et al. (1998). "Refinement of an in vitro cell model for cytochrome P450 induction." Drug Metab Dispos **26**(5): 490-6.

Soars, M. G., D. F. McGinnity, et al. (2007). "The pivotal role of hepatocytes in drug discovery." Chem Biol Interact **168**(1): 2-15.

Sogawa, K., A. Fujisawa-Sehara, et al. (1986). "Location of regulatory elements responsible for drug induction in the rat cytochrome P-450c gene." Proc Natl Acad Sci U S A **83**(21): 8044-8.

Sugano, K., Y. Nabuchi, et al. (2003). "Prediction of human intestinal permeability using

artificial membrane permeability." Int J Pharm **257**(1-2): 245-51.

Sugano, K., N. Takata, et al. (2002). "Prediction of passive intestinal absorption using bio-mimetic artificial membrane permeation assay and the paracellular pathway model." Int J Pharm **241**(2): 241-51.

Thummel, K. E. and G. R. Wilkinson (1998). "In vitro and in vivo drug interactions involving human CYP3A." Annu Rev Pharmacol Toxicol **38**: 389-430.

van De Waterbeemd, H., D. A. Smith, et al. (2001). "Property-based design: optimization of drug absorption and pharmacokinetics." J Med Chem **44**(9): 1313-33.

Vermeir, M., P. Annaert, et al. (2005). "Cell-based models to study hepatic drug metabolism and enzyme induction in humans." Expert Opin Drug Metab Toxicol **1**(1): 75-90.

Waxman, D. J. (1999). "P450 gene induction by structurally diverse xenochemicals: central role of nuclear receptors CAR, PXR, and PPAR." Arch Biochem Biophys **369**(1): 11-23.

Werlinder, V., M. Backlund, et al. (2001). "Transcriptional and post-translational regulation of CYP1A1 by primaquine." J Pharmacol Exp Ther **297**(1): 206-14.

Whitlock, J. P., Jr. (1999). "Induction of cytochrome P4501A1." Annu Rev Pharmacol Toxicol **39**: 103-25.

Whyte, J. J., C. J. Schmitt, et al. (2004). "The H4IIE cell bioassay as an indicator of dioxin-like chemicals in wildlife and the environment." Crit Rev Toxicol **34**(1): 1-83.

Wohnsland, F. and B. Faller (2001). "High-throughput permeability pH profile and high-

throughput alkane/water log P with artificial membranes." J Med Chem **44**(6): 923-30.

Youdim, K. A., C. A. Tyman, et al. (2007). "Induction of cytochrome P450: assessment in an immortalized human hepatocyte cell line (Fa2N4) using a novel higher throughput cocktail assay." Drug Metab Dispos **35**(2): 275-82.

Zhang, J. Y., Y. Wang, et al. (2006). "Xenobiotic-metabolizing enzymes in human lung." Curr Drug Metab **7**(8): 939-48.

Zheng, W., P. E. Brandish, et al. (2004). "High-throughput cell-based screening using scintillation proximity assay for the discovery of inositol phosphatase inhibitors." J Biomol Screen **9**(2): 132-40.

Zhu, C., L. Jiang, et al. (2002). "A comparative study of artificial membrane permeability assay for high throughput profiling of drug absorption potential." Eur J Med Chem **37**(5): 399-407.